




## Article – Gregory Yu. Ivanyuk memorial issue

# Compositional variation and genesis of pyrochlore, belkovite and baotite from the Sevattur carbonatite complex, India

Monojit Dey<sup>1</sup>, Sourav Bhattacharjee<sup>1</sup>, Aniket Chakrabarty<sup>1\*</sup> , Roger H. Mitchell<sup>2</sup>, Supriyo Pal<sup>3</sup>, Supratim Pal<sup>4</sup> and Amit Kumar Sen<sup>3</sup>

<sup>1</sup>Department of Earth and Climate Science, Indian Institute of Science Education and Research Tirupati, Rami Reddy Nagar, Karakambadi Road, Mangalam, Andhra Pradesh 517507, India; <sup>2</sup>Department of Geology, Lakehead University, Thunder Bay, Ontario, Canada P7B 5E1; <sup>3</sup>Department of Earth Sciences, Indian Institute of Technology Roorkee, Roorkee, Uttarakhand 247667, India; and <sup>4</sup>Department of Geology, Durgapur Government College, Durgapur, West Bengal 713214, India

### Abstract

Pyrochlore-group minerals are common in the Neoproterozoic Sevattur carbonatite complex. This complex is composed of dolomite-, calcite-, banded- and blue carbonatite together with pyroxenite, albitite and diverse syenites. This work reports the paragenetic-textural types and compositional variation of pyrochlore hosted by dolomite carbonatite, banded carbonatite and albitite together with that of alteration assemblages containing belkovite and baotite. On the basis of composition, five different types of pyrochlore are recognised and termed Pcl-I through to Pcl-V. The Pb-rich Pcl-I are present exclusively as inclusions in U-rich Pcl-IIa in dolomite carbonatite. The alteration assemblages of Pb-poor Pcl-IIB + Ba-rich or Ba-Si-rich Pcl-IV + belkovite (dolomite carbonatite) and Si-rich Pcl-V + baotite (banded carbonatite) formed after Pcl-IIa differ in these carbonatites. The albitite hosts extremely U-Ti-rich Pcl-III, mantled by Ba-rich potassium feldspar. In common with the banded carbonatite, Pcl-V is formed by alteration of Pcl-III where this mantle is partially, or completely broken. The Ba-Si-enrichment of Pcl-IV and Pcl-V together with the ubiquitous presence of baryte in all Sevattur lithologies suggests late-stage interaction with a Ba-Si-rich acidic hydrothermal fluid. This fluid was responsible for leaching silica from the associated silicates and produced Pcl-V in the silicate-rich lithologies of the banded carbonatite and albitite. The absence of Pcl-V in dolomite carbonatite is a consequence of the low modal abundance of silicates. The complex compositional diversity and lithology specific pyrochlore alteration assemblages suggest that all pyrochlore (Pcl-I to Pcl-IV) were formed initially in an unknown source and transported subsequently in their respective hosts as altered antecrysts.

**Keywords:** pyrochlore, baotite, belkovite, Sevattur carbonatite, pyrochlore alteration

(Received 8 January 2021; accepted 9 April 2021; Accepted Manuscript published online: 14 April 2021; Associate Editor: Ferdinando Bosi)

### Introduction

Pyrochlore is one of the principal sources of niobium and is found primarily in carbonatites and associated alkaline rocks such as pyroxenites, ijolites, nepheline syenites and phoscorites (Mariano, 1989; Chakhmouradian *et al.*, 2015; Mitchell, 2015). The carbonatite-hosted Brazilian deposits of Araxá and Catalão-II and the Canadian St. Honoré deposit contribute 99% of the world Nb-production (Mitchell, 2015). Pyrochlore is also found in alkaline-peralkaline granites, saturated syenites, albitites and fenites (Chakhmouradian and Mitchell, 2002).

The general formula of the pyrochlore-group mineral is  $A_2B_2X_6Y$  where:  $A$  = cubic coordination of  $Ca^{2+}$ ,  $Na^+$ ,  $K^+$ ,  $Sr^{2+}$ ,  $Ba^{2+}$ ,  $Th^{4+}$ ,  $U^{4+}$ ,  $Pb^{2+}$ ,  $Fe^{2+}$ ,  $Bi^{3+}$  and *REE* (rare earth elements)

together with vacant sites;  $B$  = octahedral coordination of Nb, Ta, Ti, Zr,  $Sb^{5+}$ , W,  $Fe^{3+}$ , Al;  $X = O, OH^-, F$ ; and  $Y = O, OH^-, F, H_2O$  and vacancies (Hogarth, 1977; Atencio *et al.*, 2010). Silicon is common in pyrochlore-group minerals, although its structural role remains ambiguous (see below). Three sub-groups are defined on the basis of the atomic proportions of Nb, Ta and Ti. These are: pyrochlore ( $Nb + Ta > 2Ti$ ;  $Nb > Ta$ ); microlite ( $Nb + Ta > 2Ti$ ;  $Ta > Nb$ ); and betafite ( $2Ti > Nb + Ta$ ) (Hogarth, 1977). In the recent Commission on New Minerals, Nomenclature and Classification (CNMNC) of the International Mineralogical Association (IMA) classification (Hatert and Burke, 2008; Atencio *et al.*, 2010), the pyrochlore group is given the status of a super group and consequently former sub-groups have been assigned to group status on the basis of the dominant-valency rule.

Regarding the crystallo-chemical role of Si in pyrochlore it has been considered by some mineralogists that Si should be considered as  $B$ -site cation (Lumpkin and Mariano, 1995; Williams *et al.*, 1997; Uher *et al.*, 1998; Chakhmouradian and Mitchell, 2002). In contrast, others have suggested that the Si is not bound structurally and is present as impurities in an amorphous or dispersed state (Voloshin *et al.*, 1989; Sorokhtina *et al.*, 2010).

\*Author for correspondence: Aniket Chakrabarty, Email: [aniket\\_chakrabarty@rediffmail.com](mailto:aniket_chakrabarty@rediffmail.com); [aniketc@iisertirupati.ac.in](mailto:aniketc@iisertirupati.ac.in)

This paper is part of a thematic set 'Alkaline Rocks' in memory of Dr. Gregory Yu. Ivanyuk

Cite this article: Dey M., Bhattacharjee S., Chakrabarty A., Mitchell R.H., Pal S., Pal S. and Sen A.K. (2021) Compositional variation and genesis of pyrochlore, belkovite and baotite from the Sevattur carbonatite complex, India. *Mineralogical Magazine* 85, 588–606. <https://doi.org/10.1180/mgm.2021.37>

Experimental studies have shown that in some instances only a minor fraction (30–50%) of the total Si occupies the *B*-site, whereas a more significant portion (50–70%) occurs in metamictised areas (Bonazzi *et al.*, 2006). A recent structural study has shown that tetrahedrally coordinated Si is present at both of the *A*- and *B*-sites affected by metamictisation (Dumańska-Słowik *et al.*, 2014).

Si-rich pyrochlore have been reported from: the Bingo carbonatite, Congo; the Prašivá massif, Slovakia; Mont Saint-Hilaire, Canada; the Gremlakha-Vyrmes massif, Kola Peninsula, Russia; and the Mariupol massif, Ukraine (Lumpkin and Mariano, 1995; Williams *et al.*, 1997; Uher *et al.*, 1998; Chakhmouradian and Mitchell, 2002; Sorokhtina *et al.*, 2010; Dumańska-Słowik *et al.*, 2014).

Pyrochlores in carbonatites are usually non-stoichiometric and never attain the ideal end-member composition of  $A_2B_2X_6Y$ . Their composition varies from  $^{[A]}(Ca, Na, U, Th, REE, Ba, Sr)_{2-x}^{[B]}(Nb, Ti, Ta, Zr, Fe^{3+})_2O_6(OH, F)_{1-y}$  in primary pyrochlore, enriched in Na, Ca and F to  $^{[A]}(Ba, Sr, REE, Pb, K, Ca, U, Th)_{\Sigma=2}^{[B]}(Nb, Ti, Ta, Zr, Fe^{3+}, Si)_2(O, OH)_6(OH, F)_{\Sigma=1} \cdot zH_2O$  in late-stage pyrochlore (Hogarth *et al.*, 2000; Zurevinski and Mitchell, 2004; Melgarejo *et al.*, 2012; Chakhmouradian *et al.*, 2015; Mitchell, 2015; Mitchell *et al.*, 2020). This compositional variation implies an increase in Ba, Sr, REE, Pb, Si, H<sub>2</sub>O and vacancies resulting in deviation from ideal stoichiometry associated with the progressive alteration of magmatic pyrochlore (Lumpkin and Ewing, 1995; Lumpkin and Mariano, 1995; Williams *et al.*, 1997; Chakhmouradian and Mitchell, 2002; Chakhmouradian *et al.*, 2015; Mitchell, 2015). Pyrochlore-group minerals are excellent indicators for characterising the ortho-, late- and post-magmatic processes affecting carbonatites and the associated rocks (Zurevinski and Mitchell, 2004; Mitchell, 2015; Walter *et al.*, 2018; Giovannini *et al.*, 2020).

In India, 26 carbonatite complexes have been reported (Krishnamurthy, 2019). Many of these complexes, such as Amba Dongar (Gujarat); Sevattur (Tamil Nadu); Beldih (West Bengal); and Samchampi (Assam) contain pyrochlore (Doroshkevich *et al.*, 2009; Viladkar and Bismayer, 2010, 2014). In this work, we report the composition and proposed genesis of diverse U-, Pb-, Ba- and Si-rich pyrochlores from the Sevattur carbonatite complex. Previously, U-rich pyrochlore with a maximum concentration of 18 wt.% UO<sub>2</sub> has been described from this complex by Viladkar and Bismayer (2014). We also describe the processes of pyrochlore alteration involving U and Nb leaching coupled with Ba and Si enrichment, leading to the formation of the rare Nb-Ti-silicates belkovite and baotite. Belkovite has been reported previously from the Vuorijärvi and Sebylavr carbonatites of the Kola Peninsula, Russia (Voloshin *et al.*, 1990; Sorokhtina *et al.*, 1998), and here we report a third occurrence from the Sevattur carbonatite complex. Additionally, we provide charge-balanced end-members for all the compositionally diverse pyrochlore-group minerals, belkovite and baotite using the 'Site Total Charge' method (Bosi *et al.*, 2019a,b). This approach makes it possible to simplify the composition of pyrochlore-group minerals and is helpful in understanding the reactions producing the pyrochlore alteration assemblages observed at Sevattur.

## Regional geology and petrography

The Neoproterozoic Sevattur carbonatite complex (12.42°N, 78.52°E) occurs as an arcuate-shaped body (~1600 × 300) m<sup>2</sup> within the NE–SW trending discontinuous Dharmapuri Shear Zone. The complex is composed of different generations of

carbonatites together with pyroxenites, diverse syenites, fenites and vermiculite-bearing mica pyroxenite (Fig. 1) (Udas and Krishnamurthy, 1970; Krishnamurthy, 1977; Subramaniam *et al.*, 1978; Viladkar and Subramaniam, 1995; Schleicher *et al.*, 1998; Ackerman *et al.*, 2017; Schleicher, 2019). The carbonatites are represented predominantly by calcite carbonatite, followed by dolomitic carbonatite and silica-rich carbonatite with minor occurrences of ankerite carbonatite (Fig. 1) (Viladkar and Subramaniam, 1995; Viladkar and Bismayer, 2014; Ackerman *et al.*, 2017). The carbonatites were emplaced during multiple intrusions as evidenced by the presence of different apatite and calcite generations hosted in the calcite and dolomite carbonatites (Schleicher, 2019). On the basis of texture, two varieties of calcite carbonatite are identified: a fine-grained variety with an average grain size between 50–500 μm; and a relatively coarse-grained variety consisting dominantly of large (>0.1–1 cm) euhedral calcite crystals. In both varieties, minor dolomite is present together with accessory apatite and magnetite. Dolomite carbonatite is medium-to-coarse grained (>0.1–10 mm) and composed of, in order of decreasing modal abundance: dolomite; calcite; apatite; minor Ba-Sr carbonates; and accessory pyrochlore (Fig. 2a,b) (Table 1).

Field observations indicate the presence of two varieties of silicate-rich carbonatite: a banded variety with alternate bands of carbonates and silicates (aegirine, magnesio-riebeckite, ferriwinchite, richterite and phlogopite) (banded carbonatite); and a blue-coloured variety (blue carbonatite) characterised by the abundant blue sodic-amphiboles and aegirine (Fig. 2c) (Table 1). The banded carbonatite is devoid of metamorphic features such as gneissosity, recrystallisation bands, and strained grains. Therefore, the banding observed is either a magmatic or a rheomorphic feature but certainly not related to post-formational metamorphic events. In both the varieties of silicate-rich carbonatite, apatite and magnetite are the typical accessory phases, whereas pyrochlore is restricted to the banded carbonatite.

The origins of these silicate-rich carbonatites remain undetermined. Similar assemblages can be found in many carbonatites which have not been metamorphosed and which are a direct consequence of magmatic differentiation from a parent carbonated silicate melt, e.g. Cargill, Canada (Pressacco, 2001; Rukhlov and Bell, 2010); Belaya Zima, Russia (Doroshkevich *et al.*, 2017); and Fen, Norway (Andersen, 1986). However, a similar assemblage could also form during multiple stages of carbonatitic magmatism as a consequence of extensive fenitisation (Elliot *et al.*, 2018). To avoid any genetic inferences and hypothetical relationships with the calcite and dolomite carbonatites we use the terminology 'banded and blue carbonatite' for these silicate-rich carbonatites.

During field investigations, we found freshly exposed albite veins cross-cutting the blue carbonatite in the western and south-eastern walls of the vermiculite mine (12.422°N, 78.528°E) (Dey *et al.*, 2021). These veins are of variable thickness (2–12 cm) and do not have surficial exposures. The veins are medium or coarse grained and composed dominantly of albite (~95 vol.%). The albite exhibits a bimodal distribution in grain size. Smaller euhedral-to-subhedral grains (~300 μm) form the majority of the matrix together with large, elongated laths (>0.5–1 cm) of macrocrysts. Other minerals present are: calcite; magnesio-riebeckite; ferriwinchite; pyrochlore; baryte; phlogopite; magnetite; and pyrite (Fig. 2e,f). Calcite and biotite occupy the interstices among the smaller albite grains and also occur as fracture fillings in the macrocrysts. Euhedral-to-subhedral blue

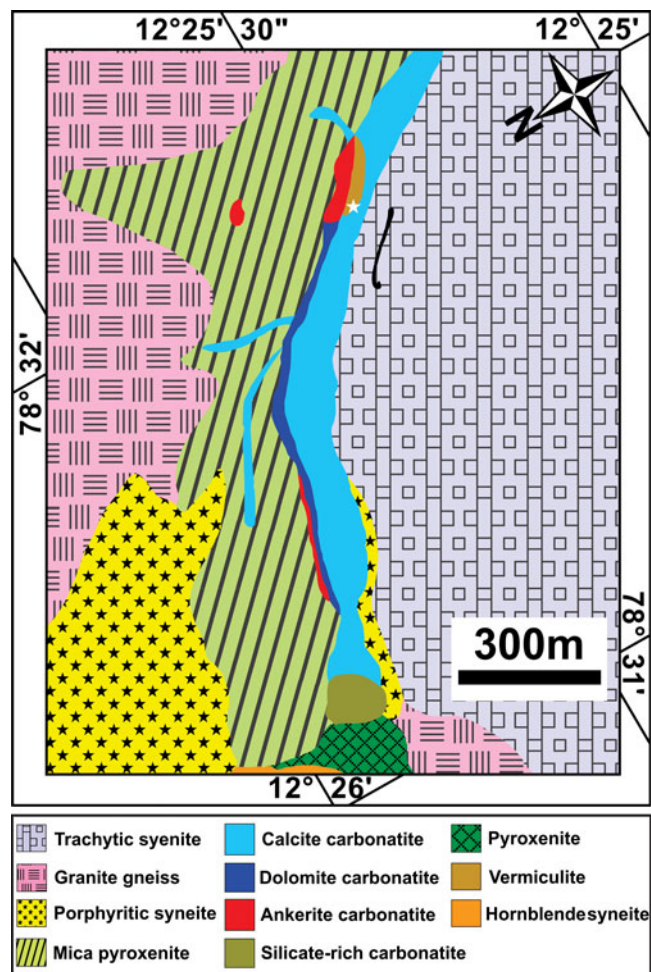


**Fig. 1.** (a) General geological map of a part of the Sevattur carbonatite complex illustrating the relations among the lithological units. The vermiculite mine is marked with a white star (modified after Ramasamy *et al.*, 2001).

amphiboles (100–300  $\mu\text{m}$ ) occur as discrete grains or in clusters within the albitite matrix.

### Experimental methods

The compositions of pyrochlore, belkovite and baotite were determined using a CAMECA SX100 electron microprobe (EMP) at the Institute Instrumentation Centre (IIC), Indian Institute of Technology Roorkee. This instrument is equipped with four wavelength dispersive (WD) spectrometers and one energy dispersive (ED) spectrometer. Analyses were undertaken with a 20 kV accelerating voltage, 10 nA beam current and a focussed 1–10  $\mu\text{m}$  beam diameter depending on the size of the mineral analysed. Prior to EMP data collection, the polished sections were examined in transmitted light microscope. Selection of analytical points was guided by back-scattered electron (BSE) images. The following X-ray lines and standards were used for quantification of the major elements: Nb-metal ( $\text{NbL}\alpha$ ), Ta metal ( $\text{TaM}\alpha$ ),  $\text{UO}_2$  ( $\text{UM}\alpha$ ),  $\text{ThO}_2$  ( $\text{ThM}\alpha$ ), zircon ( $\text{ZrL}\alpha$ ), jadeite ( $\text{Si-K}\alpha$ ), rutile ( $\text{TiK}\alpha$ ), jadeite ( $\text{AlK}\alpha$ ), baryte ( $\text{BaL}\alpha$ ), celestine ( $\text{SrL}\alpha$ ), galena ( $\text{PbK}\alpha$ ), hematite ( $\text{FeK}\alpha$ ), rhodonite ( $\text{MnK}\alpha$ ), periclase ( $\text{MgK}\alpha$ ), diopside ( $\text{CaK}\alpha$ ), jadeite ( $\text{NaK}\alpha$ ), orthoclase ( $\text{KK}\alpha$ ), fluorite ( $\text{FK}\alpha$ ) and synthetic REE glass ( $\text{LaL}\alpha$ ,  $\text{CeL}\alpha$ ,  $\text{PrL}\alpha$ ,  $\text{NdL}\alpha$ ,  $\text{SmL}\alpha$ ,  $\text{EuL}\alpha$ ,  $\text{GdL}\alpha$ ,  $\text{TbL}\beta$ ,  $\text{DyL}\alpha$ ,  $\text{HoL}\alpha$ ,  $\text{ErL}\alpha$ ,  $\text{TmL}\alpha$ ,  $\text{YbL}\alpha$

and  $\text{LuL}\alpha$ ). The precision of the analyses from the repeated analysis of standards suggests that standard deviation is less than  $\pm 0.5\%$  for major, and less than 0.1% for minor elements. Peak counting times for major elements were 10–20 s and 30–60 s for minor elements (half of the values for the background), with shorter times for volatile elements.

Additional analyses of pyrochlore, baotite and belkovite were carried out at Lakehead University, Canada by quantitative X-ray energy dispersive spectrometry (EDS) using a Hitachi FE-SU70 scanning electron microscope equipped with AZtec software (Oxford Instruments). An accelerating voltage of 20 kV and beam current of 0.3 nA were used to collect X-ray spectra for 120 s for all the major elements. For F, a  $\text{CaF}_2$  standard was used with a collection time of 250 s. Analytical standards used for calibration were: apatite (P, Ca);  $\text{SrTiO}_3$  (Sr, Ti);  $\text{ThNb}_4\text{O}_{12}$  (Th, Nb); Mn-rich fayalite (Mn, Fe, Mg and Si); wollastonite (Si, to ratify the excess silica in belkovite); jadeite (Na, Al); benitoite (Ba, Ti); REE phosphate glasses; Ta and U metals (Mitchell and Smith, 2017). Any Na-bearing minerals were analysed with a beam rastered over areas ranging from 100 to 1000  $\mu\text{m}^2$  to minimise Na volatilisation.

### Pyrochlore – composition and parageneses

On the basis of their composition, two main types of pyrochlore are present at Sevattur. Pyrochlore hosted in dolomite and banded carbonatites are characterised by elevated Ta contents (up to 13.4 wt.%  $\text{Ta}_2\text{O}_5$ ), whereas those present in albitite are essentially Ta poor (<1 wt.%  $\text{Ta}_2\text{O}_5$ ). The silicate-rich blue carbonatite is devoid of pyrochlore. Carbonatite-hosted pyrochlores are relatively large (0.1–1 mm) (Fig. 2a–c), whereas the majority of the albitite-hosted pyrochlores (Dey *et al.*, 2021) are small (<50  $\mu\text{m}$ ), and large grains (>100  $\mu\text{m}$ ) are seldom present (Fig. 2d–f). The habit of these pyrochlores are variable, ranging from anhedral (Fig. 2a) to subhedral (Fig. 2c). They appear lemon-yellow to orange/brown in plane polarised light (Fig. 2a–f). These pyrochlores are also characterised by a mantle of Ba-bearing potassium feldspar (Dey *et al.*, 2021) (Fig. 2d). However, there are few examples in which this mantle is partly or entirely disrupted. In albitite, pyrochlores are also present as inclusions in amphibole (Fig. 2e,f), implying that these amphiboles postdate pyrochlore formation.

On the basis of texture and compositional variation, we have identified five types of pyrochlore in the carbonatites and albitite: Pcl-I to Pcl-V (Fig. 3a–h).

#### Pyrochlore-I

Back-scattered electron images show that Pcl-I occurs exclusively as high-AZ (AZ: average atomic number) inclusions (<5  $\mu\text{m}$ ) within Pcl-II (>50  $\mu\text{m}$ ) of intermediate-AZ (Fig. 3a,b). Compositionally, Pcl-I is characterised by high Pb [20.4–21.0 wt.%  $\text{PbO}$ ; 0.50–0.58 atoms per formula unit (apfu)], relatively low contents of U (up to 20.5 wt.%  $\text{UO}_2$ ), Nb (30.1–32.7 wt.%  $\text{Nb}_2\text{O}_5$ ), Ta (5.1–6.2 wt.%  $\text{Ta}_2\text{O}_5$ ) and Ti (2.9–4.8 wt.%  $\text{TiO}_2$ ), with Ca (1.5–2.2 wt.%  $\text{CaO}$ ) (Fig. 4) (Table 2). Pcl-I have minor Ba, Fe and Sr contents.

#### Pyrochlore-II

Pcl-II occurs either as hosts to Pcl-I or associated with later generation Pcl-IV and Pcl-V. The Pcl-II is devoid of any BSE-detectable primary zoning and characterised by patchy



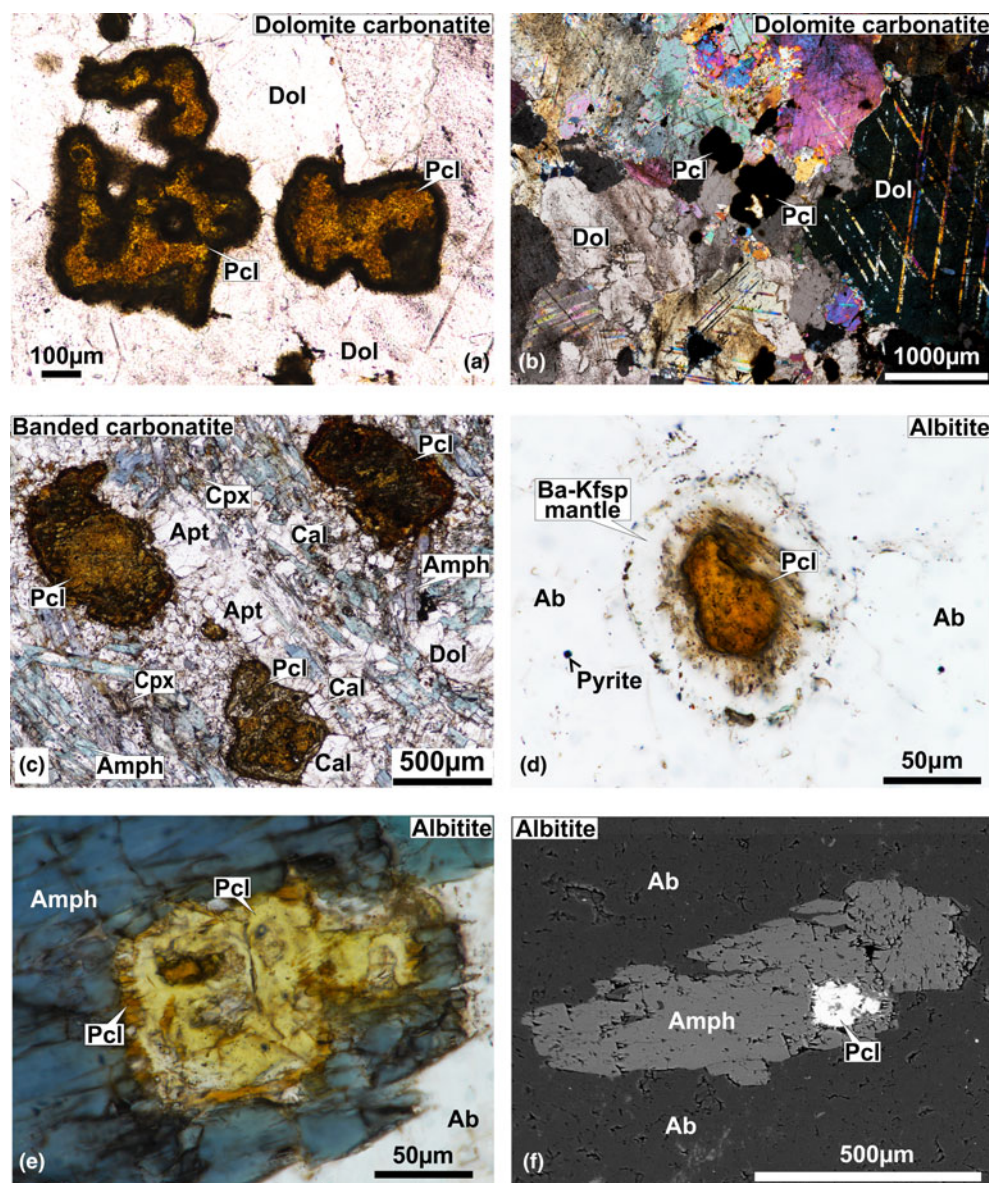


**Fig. 2.** Transmitted light (a–e) and back-scattered electron (BSE) images (f) of pyrochlore and associated minerals from Sevattur. Photomicrographs of anhedral-subhedral pyrochlore (Pcl) grains within the dolomite (Dol) matrix in dolomite carbonatite in plane polarised light (PPL) (a) and cross polarised light (b). (c) PPL photomicrograph illustrating clusters of pyrochlore grains associated with calcite (Cal), clinopyroxene (Cpx), amphibole (Amph) and apatite (Apt) in a dolomite (Dol) matrix in banded carbonatite. Note the late-formed, elongated and acicular blue-green amphiboles (Amph). (d) Albitite-hosted pyrochlore crystal with a thick orbicular mantle of Ba-rich potassium feldspar (Ba-Kfsp) (PPL image). (e) An amphibole surrounding an inclusion of pyrochlore with a lemon-yellow core and orange coloured rim, in albitite (PPL image). (f) Back-scattered electron (BSE) image of the same amphibole and pyrochlore crystals as in (e).

zoning together with numerous fractures extending from the rim towards the core (Fig. 3a,b). In general, Pcl-II are anhedral and characterised by extensive post-formational alteration resulting in diverse low- and intermediate-AZ zones (Fig. 3a,b). On the basis of compositional variation, Pcl-II is further subdivided into Pcl-IIa and Pcl-IIb (Fig. 3a). The Pcl-IIa is present in dolomite and banded carbonatite, whereas Pcl-IIb is restricted to dolomite carbonatite as low-AZ areas in marginal parts of Pcl-IIa (Fig. 3a). Pcl-IIa, unlike Pcl-I, is characterised by low Pb contents (1.5–2.2 wt.% PbO; 0.03–0.05 apfu) and a higher concentration of U (up to 30.7 wt.%  $\text{UO}_2$ ), Nb (28.3–39.7 wt.%  $\text{Nb}_2\text{O}_5$ ), Ta (6.2–8.8 wt.%  $\text{Ta}_2\text{O}_5$ ), Ti (3.6–12.2 wt.%  $\text{TiO}_2$ ) and Ca (3.8–7.2 wt.% CaO) (Table 2) (Fig. 4). Pcl-IIa also have minor Ba, Fe and Sr contents. In contrast, Pcl-IIb is relatively poorer in U (11.7–17.1 wt.%

$\text{UO}_2$ ), Nb (28.4–30.2 wt.%  $\text{Nb}_2\text{O}_5$ ), Ca (3.8–4.1 wt.% CaO) and Ti (3.8–4.0 wt.%  $\text{TiO}_2$ ) with high Ta (up to 12.8 wt.%  $\text{Ta}_2\text{O}_5$ ) and Si (4.9–6.4 wt.%  $\text{SiO}_2$ ) contents (Table 2) (Fig. 4).

### Pyrochlore-III

Albitite-hosted U-rich pyrochlore (Pcl-III) with Ba-potassium feldspar mantles has been described in detail by Dey *et al.* (2021), and only a summary of this paragenesis is included in this work for comparison with pyrochlore occurring in the associated carbonatites. These pyrochlore are restricted to albitite and present in two textural modes: either surrounded by an orbicular mantle of Ba-bearing potassium feldspar; or as an inclusion within the amphibole (Figs 2f, 3d). In places, this mantle is

**Table 1.** Mineral assemblages in different lithological units.

Rock types	Major minerals	Accessory minerals
Calcite carbonatite Dolomite carbonatite	Calcite + Sr-Mg calcite + dolomite ± richterite ± ferri-winchite ± phlogopite Dolomite + calcite + Ba-Sr carbonates	Apatite ± magnetite Apatite + pyrochlore (Pcl-I, IIa, IIb & IV) + belkovite + magnetite ± fluorite
Banded carbonatite	Dolomite + calcite + magnesio-riebeckite + ferri-winchite + richterite ± actinolite ± tremolite + aegirine + phlogopite	Apatite + pyrochlore (Pcl-IIa & V) + baotite + magnetite
Blue carbonatite	Dolomite + calcite + magnesio-riebeckite + magnesio-arfvedsonite + aegirine + phlogopite	Apatite + magnetite + albite + quartz + baryte + zircon + rutile
Pyroxenite Albitite	Diopside + magnesio-hastingsite + biotite + calcite Albite + calcite + orthoclase + magnesio-riebeckite + ferri-winchite + phlogopite	Apatite + magnetite + ilmenite ± titanite Pyrochlore (Pcl-III & V) + magnetite + pyrite + galena + baryte

partially disrupted leading to extensive metamictisation together with alteration resulting in the formation of U-poor Si-rich pyrochlore (Pcl-V). Compositionally, Pcl-III (comparable to 'Pcl-II' of Dey *et al.*, 2021) is characterised by a very high U content (31–33.1 wt.% UO<sub>2</sub>; 0.49–0.53 apfu) compared to other pyrochlore (Table 2). Pcl-III is also enriched in Ti, Ca and Na (11.7–14.0 wt.% TiO<sub>2</sub>; 5.5–10.3 wt.% CaO; 0.9–1.8 wt.% Na<sub>2</sub>O) (Table 2) and depleted in Ba (3.7–5.7 wt.% BaO) compared to Pcl-I and Pcl-II, whereas the Nb content is comparable to that of Pcl-II. Minor amounts of Si, Pb, Sr and Fe are also present in Pcl-III (Table 2). It is noteworthy that the Pcl-III is relatively less-altered compared to other pyrochlore types and the effects of metamictisation appear to be minimal as evidenced in BSE images (Fig. 3b).

#### Pyrochlore-IV

Pcl-IV are present in the dolomite carbonatite in association with belkovite (Fig. 3c,e). BSE imagery reveals that majority of the Pcl-IV are partially altered and characterised by patchy zoning with variable high- and low-AZ areas resulting from variations in the A-site cation abundances of Ba and U (Fig. 3e) (Table 2; compositions 11 and 14). In some cases, the Pcl-IV grains are extensively metamictised with profuse development of fractures making them prone to alteration (Fig. 3f). Such grains are characterised by a U-rich (high-AZ) relict core and U contents gradually decrease towards the rim (low-AZ), coupled with progressive enrichment in Ba and Si (Fig. 3f) (Table 2; compositions 12, 13). Extreme compositional variation of these pyrochlore is evident from the variable Ta (2.0–9.1 wt.% Ta<sub>2</sub>O<sub>5</sub>), Si (1.2–10.7 wt.% SiO<sub>2</sub>), U (28.3–4.9 wt.% UO<sub>2</sub>) and Pb (0.4–4.3 wt.% PbO) (Table 2) contents together with only minor Ca, Sr and Fe. Moreover, Pcl-IV has relatively higher A-site vacancies (0.6–1.3 pfu) compared to Pcl-I, -II and -III. Pyrochlore-IV is enriched in Ba and Nb (8.9–23.9 wt.% BaO; 34.9–41.0 wt.% Nb<sub>2</sub>O<sub>5</sub>) (Table 2) relative to all other Sevattur pyrochlore.

#### Pyrochlore-V

The silica-rich Pcl-V is found in the banded carbonatite and albitite. In the banded carbonatite it occurs as low-AZ patches in association with Pcl-IIa (Fig. 3g) and discrete grains are absent. In contrast, Pcl-V in albitite is present either as a discrete grain or in association with Pcl-III, where the orbicular mantle is partially or completely disrupted (Fig. 3h). Texturally, pyrochlore-V are characterised by numerous fractures related to extensive metamictisation resulting in patchy zoning similar to that exhibited by

Pcl-IV (Fig. 3g,h). These pyrochlore are characterised by a high Si content (12.6–24.9 wt.% SiO<sub>2</sub>; 0.72–1 apfu) together with low Nb and U (20.9–27.1 wt.% Nb<sub>2</sub>O<sub>5</sub>; 13.3–19.4 wt.% UO<sub>2</sub>) (Table 2) contents compared to Pcl-I to Pcl-III; with a variable Ca (4.3–7.0 wt.% CaO) content. It is noteworthy that the Pcl-IIa and Pcl-III associated with Pcl-V in the banded carbonatite and albitite, are essentially U and Nb rich and Si poor (Table 2). However, all Pcl-V are essentially Si rich and U-Nb poor suggesting a significant loss in Nb and U during the alteration of the precursor pyrochlore. Depending on the host lithology, Pcl-V can be further subdivided into Si-Ti-rich (Table 2; compositions 16–18) and Si-Ta-rich varieties (Table 2; compositions 19, 20) present in the albitite and carbonatite, respectively. Pcl-V in albitite are relatively Ba, Al, K and Na rich compared to those present in the banded carbonatite. In general, Pcl-V are characterised by more A-site vacancies (>1 pfu, Table 2) relative to other pyrochlore.

### Minerals formed by alteration of pyrochlore

#### Belkovite

Belkovite [Ba<sub>3</sub>Nb<sub>6</sub>(Si<sub>2</sub>O<sub>7</sub>)<sub>2</sub>O<sub>12</sub>] is a rare sorosilicate which has been reported from the Vuorijärvi and Seblyavr carbonatite complexes (Kola Peninsula, Russia) as a late-stage alteration product of Ba-rich pyrochlore (Voloshin *et al.*, 1991; Sorokhtina *et al.*, 1998). In common with the Vuorijärvi occurrence, belkovite found at Sevattur is present only within an assemblage consisting of U-rich Pcl-IIa (high-AZ), Ba-rich Pcl-IV (low-AZ), baryte and Ba-Sr carbonates in dolomite carbonatite (Figs 3c, 5a–e). BSE imagery shows that belkovite is restricted mainly to intensely metamictised areas of Pcl-IV containing numerous fractures (Fig. 5b–e). The associated U-rich Pcl-IIa are present as relict patches within this assemblage (Fig. 5c–e). The association of belkovite with Si-rich Pcl-IV suggests it forms as an alteration product of these pyrochlores.

Sevattur belkovite is similar in composition to that of the Vuorijärvi occurrence (Voloshin *et al.*, 1991), being enriched in Nb (41.6–42.5 wt.% Nb<sub>2</sub>O<sub>5</sub>), Ba (30.8–32.1 wt.% BaO) and Si (17.3–17.4 wt.% SiO<sub>2</sub>) together with, in order of decreasing abundance, minor amounts of Ti, Ta, Fe, Sn, K and Na (Table 3; compositions 1–4). Because of the high degree of metamictisation, Pcl-IV has low 4.87 wt.% UO<sub>2</sub> (Table 2; composition 15) contents compared to those of less-altered Pcl-IIa (up to 25.7 wt.% UO<sub>2</sub>; Table 2; composition 4) (Fig. 4). Thus, alteration of Pcl-IIa to Pcl-IV and belkovite is indicative of significant U mobilisation.



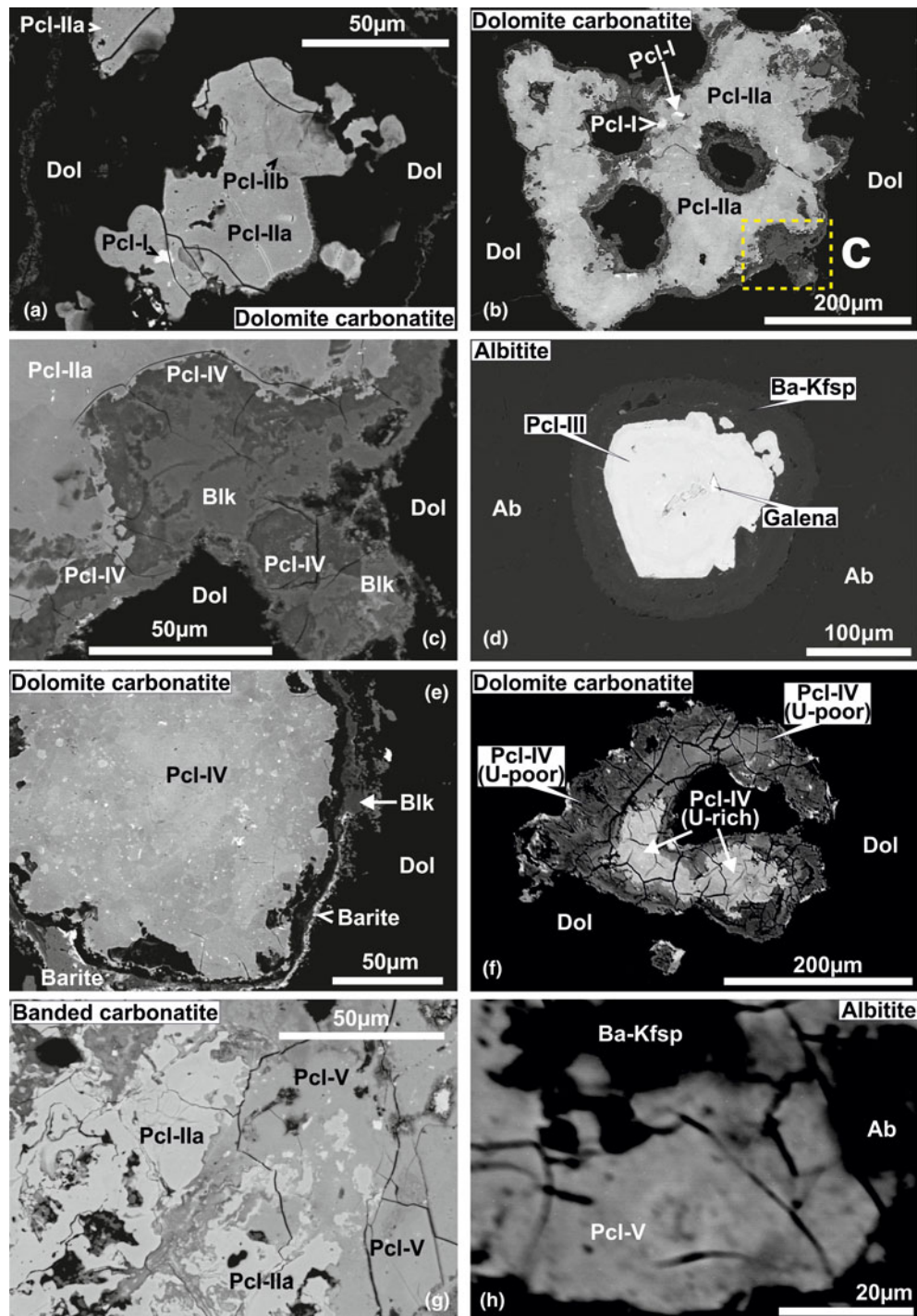


**Fig. 3.** BSE images illustrating the different textural modes of occurrences of pyrochlore-group minerals at Sevattur. (a) Pb-rich Pcl-I inclusions (high-AZ; AZ: average atomic weight) within U-rich Pcl-IIa (intermediate-AZ). Note that Pcl-IIb is formed by alteration of Pcl-I and Pcl-IIa along the grain margin (low-AZ areas). (b) and (c) Anhedra Pcl-IIa with variable AZ areas illustrating patchy zoning. Note the extensive alteration along the grain margin. (c) Enlarged view of a part of the altered grain margin (dashed lines in (b)); the alteration assemblage of Ba-rich Pcl-IV and belkovite (Blk) formed after Pcl-IIa. (d) A high-AZ U-Ti-rich euhedral Pcl-III crystal with an inclusion of galena, mantled by low-AZ Ba-rich potassium feldspar (Ba-Kfsp). (e) Pcl-IV in association with belkovite (low-AZ) and baryte (high-AZ) along the grain margin in dolomite carbonatite. Note the variable AZ areas in Pcl-IV illustrating patchy zoning. (f) A highly metamictised and fractured Pcl-IV with a relict U-rich core (high-AZ) and U-poor rim (low-AZ) in dolomite carbonatite. (g) An extensively metamictised grain of Pcl-IIa replaced by late-stage Si-rich Pcl-V in banded carbonatite. Note the relict patches of relatively unaltered Pcl-IIa. (h) Partially-disrupted Ba-rich potassium feldspar (Ba-Kfsp) mantle facilitating the formation of Pcl-V in albitite.

### Baotite

Baotite, is a chlorine-bearing Ba-Ti-Nb cyclosilicate [ $\text{Ba}_4(\text{Ti},\text{Nb},\text{Fe})_8\text{Si}_4\text{O}_{28}\text{Cl}$ ] first reported from hydrothermal quartz veins at

Bayan-Obo, Mongolia, China (Peng, 1959; Semenov *et al.*, 1961). Baotite occurs in alkaline-peralkaline rocks and carbonatites as a late-stage mineral with compositions varying between the end-members  $\text{Ba}_4\text{Ti}_8\text{Si}_4\text{O}_{28}\text{Cl}$  and  $\text{Ba}_4\text{Ti}_2\text{Fe}_2\text{Nb}_4\text{Si}_4\text{O}_{28}\text{Cl}$

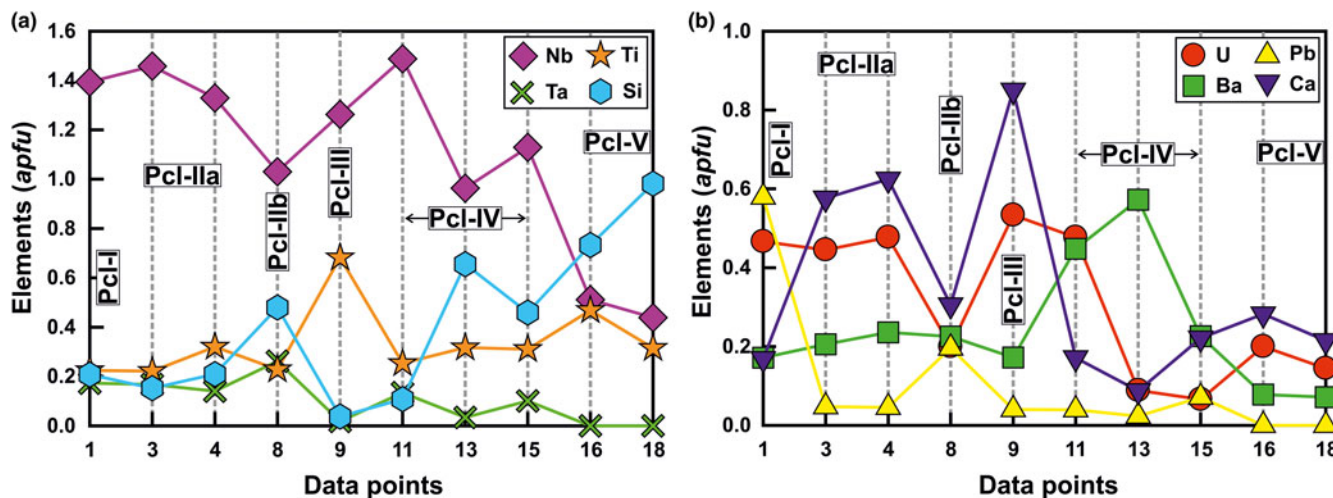


**Fig. 4.** The compositional variation (apfu) of different pyrochlore types (Pcl-I to Pcl-V) from the Sevattur carbonatite complex illustrating elemental concentrations of B-site (a) and A-site cations (b) respectively. Note that the relatively unaltered pyrochlore (Pcl-IIa and Pcl-III) are rich in Nb, Ca and U compared to the late-formed Pcl-IIb, -IV and -V. The later pyrochlore are essentially Ba- or Ba-Si-enriched.

(Cooper, 1996; Potter and Mitchell, 2005; Kullerud *et al.*, 2012). Baotite occurs in lamproites, alkali-granite/alkaline pegmatites, and alkaline metasomatites and is usually rich in Ti (Fig. 6) (Kullerud *et al.*, 2012; Kaur and Mitchell, 2019, and references therein). In India, the only reported occurrence is from the Gundrapalli lamproite, Telangana (Kaur and Mitchell, 2019) (Fig. 6). In general, baotite is rare in carbonatites with notable examples being in the Haast River (New Zealand) and Lueshe (Congo) carbonatite complexes (Cooper, 1996; Wall *et al.*, 1996). In these occurrences, baotite is present as an accessory phase in late-stage ferroan dolomite (ankerite)-, siderite- and carbothermal carbonatites. They are rich in Nb and Fe relative to Ti (Fig. 6).

At Sevattur, baotite is present in trace amounts as anhedral grains (~50  $\mu\text{m}$ ) restricted to the banded carbonatite. BSE imagery shows baotite occurs as low-AZ areas along the metamictised grain margins of Pcl-IIa, associated with an unidentified U-Nb-rich phase (63.7 wt.%  $\text{UO}_2$ , 18.6 wt.%  $\text{Nb}_2\text{O}_5$ ) (Supplementary material 3) (Fig. 5f,g). Sevattur baotite is rich in Ba (30.2–33.8 wt.% BaO), Nb (25.4–27.6 wt.%  $\text{Nb}_2\text{O}_5$ ), Ti (13.0–14.5 wt.%  $\text{TiO}_2$ ), Fe (5.4–6.6 wt.% FeO) and Si (13.0–13.8 wt.%  $\text{SiO}_2$ ) with Cl contents varying between 0.7 and 0.9 apfu (Table 3; compositions 5–7).

## Pyrochlore, belkovite and baotite – classification and nomenclature

### Pyrochlore

The majority of Sevattur pyrochlore are characterised by Nb > Ti or Ta (apfu) and are classified as pyrochlore *sensu stricto* in the Nb–Ta–Ti ternary diagram (Hogarth 1977, Atencio *et al.*, 2010) (Fig. 7a). However,  $\text{Si}^{4+}$  is the dominant valence cation at the B-site of Pcl-V (Table 2, compositions 16–20) (Fig. 7b). In the IMA–CNMNC pyrochlore classification no element other than  $\text{Ti}^{4+}$  (betafite) is assigned to this tetravalent ( $M^{4+}$ ) site (Atencio *et al.*, 2010). Hence, using the IMA nomenclature, the classification of Si-rich Pcl-V pyrochlore (Fig. 7b) might require the establishment of a new member of the pyrochlore supergroup. A similar problem arises in using the IMA nomenclature in

classifying Zr-pyrochlore from the Guaniamo kimberlite, Venezuela (Sharygin *et al.*, 2009). However, establishing a Si-dominant group of the pyrochlore supergroup is not feasible as the crystal-chemical role of Si in the pyrochlore structure is debatable (Bonazzi *et al.*, 2006; Dumańska-Słowik *et al.*, 2014). The silicified pyrochlores from the Mariupol massif showed that the Si could not be present in octahedral coordination, and the pyrochlore formula is calculated excluding Si as a B-site cation (Dumańska-Słowik *et al.*, 2014). Texturally, these pyrochlores are relatively unaltered, as evidenced by their euhedral habit and relict oscillatory zoning, which was overprinted by patchy zoning. In contrast, Sevattur pyrochlores are subhedral-to-anhedral in shape with intense patchy zonation and characterised by distinctive alteration assemblages. Significantly, Mariupol pyrochlores with a very low U content (0.23–3.14 wt.%  $\text{UO}_2$ ) and relatively higher Na and F contents (Dumańska-Słowik *et al.*, 2014) are not directly comparable to those found at Sevattur. Thus, it is evident that the effect of metamictisation is far more intense at Sevattur compared to the silicified pyrochlores from the Mariupol massif. However, following the pyrochlore formula calculation of Dumańska-Słowik *et al.* (2014) we find that some of our analyses with a low  $\text{SiO}_2$  result in an overestimation of total oxygens (>7 apfu). In several instances, complications arise for altered pyrochlores (Pcl-IV and Pcl-V) with low analytical totals, leading to a low A-site vacancy with near ideal total oxygen. These anomalies cannot be justified as progressive alterations of pyrochlores usually results in significant A- and Y-site vacancies. This probably suggests that some Si might be present as B-site cation. A similar observation was made by Bonazzi *et al.* (2006) from the pyrochlores of the Narssârssuk nepheline syenites, Greenland. Consequently, we consider Si as a B-site cation and pyrochlore formula is calculated accordingly as suggested by the IMA (Atencio *et al.*, 2010).

The IMA pyrochlore nomenclature is based on the ‘dominant-valency rule’, whereas the previous classification (Hogarth, 1977) was based on the ‘dominant constituent’ at the A-site excepting Ca and Na. The IMA scheme leads to many problems (discussed below) when used for petrogenetic purposes, and in particular for the non-stoichiometric pyrochlore found at Sevattur. To illustrate the nomenclatural problems, we have used both the Hogarth

**Table 2.** Representative pyrochlore compositions.

Wt.%	DC 1	DC 2	DC 3	DC 4	BC 5	BC 6	DC 7	DC 8	Abt 9	Abt 10	DC 11	DC 12	DC 13	DC 14	DC 15	Abt 16	Abt 17	Abt 18	BC 19	BC 20
Na <sub>2</sub> O	bdl	bdl	bdl	bdl	bdl	0.62	bdl	bdl	1.76	0.94	0.33	0.13	0.18	bdl	bdl	1.89	1.31	1.37	0.41	bdl
K <sub>2</sub> O	bdl	bdl	bdl	bdl	bdl	bdl	bdl	bdl	bdl	0.14	bdl	bdl	bdl	bdl	bdl	0.69	2.48	1.24	bdl	bdl
MgO	bdl	bdl	bdl	bdl	bdl	bdl	bdl	bdl	bdl	0.06	bdl	0.08	0.32	bdl	bdl	0.60	0.57	2.35	bdl	bdl
CaO	1.54	2.15	6.63	6.98	3.75	5.64	4.15	3.78	10.27	5.49	1.82	2.51	1.34	2.13	3.39	5.62	4.74	4.32	6.79	6.97
MnO	bdl	bdl	bdl	bdl	bdl	bdl	bdl	bdl	bdl	0.10	0.01	bdl	bdl	bdl	bdl	0.02	bdl	0.52	bdl	bdl
FeO	1.98	1.38	2.85	2.30	1.26	3.49	3.34	3.07	bdl	1.77	1.64	2.11	4.51	0.43	1.85	1.69	1.57	4.85	1.85	2.17
SrO	1.43	1.67	3.45	3.21	1.41	4.76	3.01	2.31	1.09	bdl	1.53	2.95	1.39	1.86	1.07	bdl	bdl	bdl	1.74	1.35
BaO	4.28	3.37	6.46	7.21	2.19	2.47	6.36	7.62	5.69	3.67	13.00	15.84	23.92	8.89	9.48	4.25	4.77	3.94	3.83	3.40
PbO	21.01	20.39	2.17	2.03	1.54	1.62	11.08	9.65	1.93	bdl	1.67	0.40	1.42	1.68	4.34	bdl	bdl	bdl	4.00	4.39
ThO <sub>2</sub>	bdl	bdl	bdl	bdl	0.59	bdl	0.15	bdl	bdl	bdl	bdl	bdl	bdl	bdl	bdl	bdl	bdl	bdl	bdl	bdl
UO <sub>2</sub>	20.46	20.44	24.64	25.67	30.72	29.27	17.07	11.89	31.02	33.11	24.38	17.50	6.52	28.31	4.87	19.40	15.69	14.00	13.27	14.32
Al <sub>2</sub> O <sub>3</sub>	bdl	bdl	bdl	bdl	bdl	bdl	bdl	bdl	bdl	0.29	0.16	0.29	0.42	bdl	bdl	5.19	6.41	4.84	bdl	bdl
SiO <sub>2</sub>	2.03	2.43	1.88	2.51	3.41	1.71	4.89	6.36	0.49	1.78	1.23	10.43	10.73	1.63	7.54	15.62	24.89	21.17	12.59	12.69
TiO <sub>2</sub>	2.92	4.76	3.63	5.10	12.23	9.68	3.79	4.02	11.73	14.00	3.83	2.80	6.90	3.66	6.78	13.27	10.45	9.04	8.30	8.42
Nb <sub>2</sub> O <sub>5</sub>	30.12	32.65	39.74	35.21	28.34	30.35	28.43	30.19	36.15	36.06	37.44	34.68	34.89	39.27	41.01	24.11	22.46	20.92	27.12	24.15
Ta <sub>2</sub> O <sub>5</sub>	6.22	5.07	7.59	6.19	7.40	8.82	10.62	12.76	0.85	bdl	5.61	4.04	2.04	9.13	6.10	bdl	bdl	bdl	13.40	12.72
F	bdl	bdl	bdl	bdl	bdl	bdl	bdl	bdl	bdl	bdl	bdl	bdl	bdl	bdl	bdl	bdl	bdl	bdl	bdl	bdl
Total	91.99	94.31	99.04	96.41	92.84	98.43	92.89	91.65	100.98	97.41	92.65	93.76	94.58	96.99	86.43	92.35	95.34	88.56	93.30	90.58
O≡F	-	-	-	-	-	-	-	-	-	-	-	-	-	-	-	-	-	-	-	-
Sum	91.99	94.31	99.04	96.41	92.84	98.43	92.89	91.65	100.98	97.41	92.65	93.76	94.58	96.99	86.43	92.35	95.34	88.56	93.30	90.58
Atoms per formula unit calculated on the basis of sum of B cations = 2																				
Na	-	-	-	-	-	0.096	-	-	0.264	0.126	0.056	0.017	0.021	-	-	0.172	0.101	0.123	0.046	-
K	-	-	-	-	-	-	-	-	-	0.012	-	-	-	-	-	0.041	0.125	0.073	-	-
Mg	-	-	-	-	-	-	-	-	-	0.006	-	0.008	0.029	-	-	0.042	0.034	0.162	-	-
Ca	0.169	0.208	0.577	0.625	0.293	0.481	0.379	0.306	0.850	0.406	0.171	0.181	0.088	0.185	0.221	0.283	0.201	0.215	0.419	0.447
Mn	-	-	-	-	-	-	-	-	-	0.006	0.001	-	-	-	-	0.001	-	0.020	-	-
Fe <sup>2+</sup>	0.170	0.104	0.193	0.161	0.077	0.232	0.238	0.194	-	0.102	0.121	0.119	0.230	0.029	0.094	0.066	0.052	0.188	0.089	0.109
Sr	0.085	0.087	0.162	0.155	0.060	0.220	0.149	0.101	0.049	-	0.078	0.115	0.049	0.088	0.038	-	-	-	0.058	0.047
Ba	0.172	0.119	0.205	0.236	0.063	0.077	0.212	0.225	0.172	0.099	0.448	0.419	0.573	0.283	0.226	0.078	0.074	0.072	0.086	0.080
Pb	0.579	0.496	0.047	0.046	0.030	0.035	0.254	0.196	0.040	-	0.040	0.007	0.023	0.037	0.071	-	-	-	0.062	0.071
Th	-	-	-	-	0.010	-	0.003	-	-	-	-	-	-	-	-	-	-	-	-	-
U	0.466	0.411	0.445	0.477	0.498	0.519	0.323	0.200	0.533	0.509	0.477	0.263	0.089	0.512	0.066	0.200	0.138	0.144	0.170	0.191
ΣA	1.641	1.425	1.629	1.700	1.031	1.660	1.558	1.222	1.908	1.266	1.392	1.129	1.102	1.134	0.716	0.883	0.725	0.997	0.930	0.945
□A	0.359	0.575	0.371	0.300	0.969	0.340	0.442	0.778	0.092	0.734	0.608	0.871	0.898	0.866	1.284	1.117	1.275	1.003	1.070	1.055
Al	-	-	-	-	-	-	-	-	-	0.024	0.017	0.023	0.030	-	-	0.287	0.299	0.264	-	-
Si	0.208	0.220	0.153	0.210	0.249	0.136	0.416	0.480	0.038	0.123	0.108	0.704	0.656	0.132	0.459	0.733	0.987	0.982	0.725	0.760
Ti	0.225	0.323	0.222	0.320	0.671	0.580	0.243	0.228	0.682	0.727	0.253	0.142	0.317	0.224	0.311	0.468	0.312	0.315	0.359	0.379
Nb	1.394	1.333	1.457	1.329	0.934	1.093	1.095	1.030	1.262	1.126	1.488	1.057	0.963	1.442	1.129	0.512	0.402	0.439	0.706	0.654
Ta	0.173	0.124	0.168	0.141	0.146	0.191	0.246	0.262	0.018	-	0.134	0.074	0.034	0.202	0.101	-	-	-	0.210	0.207
ΣB	2.000	2.000	2.000	2.000	2.000	2.000	2.000	2.000	2.000	2.000	2.000	2.000	2.000	2.000	2.000	2.000	2.000	2.000	2.000	2.000
F	-	-	-	-	-	-	-	-	-	-	-	-	-	-	-	-	-	-	-	-
O (calc)	6.890	6.564	6.888	6.911	6.079	6.773	6.555	6.067	6.950	6.258	6.643	5.938	5.664	6.467	5.398	5.094	4.802	5.131	5.535	5.565

1–2: pyrochlore-I; 3–6: pyrochlore-IIa; 7–8: pyrochlore-IIb; 9–10: pyrochlore-III; 11–15: pyrochlore-IV; 16–20: pyrochlore-V. Compositions 1–9, 14, 15, 19, 20: ED X-ray spectrometry (Lakehead University) and 10–13, 16–18: WD electron microprobe (IIT Roorkee)

bdl: below detection limit

DC: dolomite carbonatite; BC: banded carbonatite; Abt: albitite



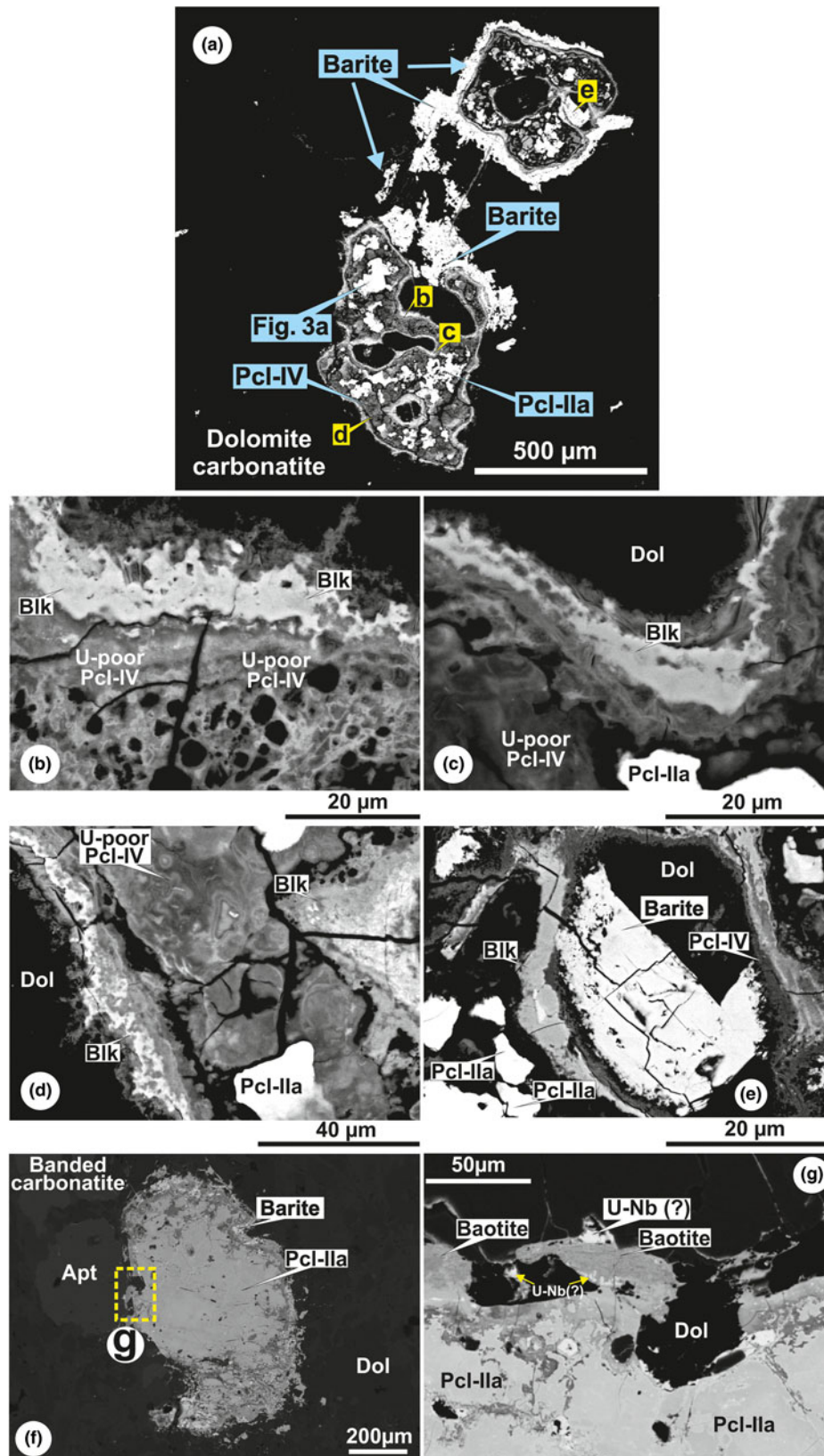


**Fig. 5.** BSE images showing the lithology specific alteration assemblages in dolomite (a–e) and banded (f–g) carbonatite. (a) A complex association of Pcl-IIa, Pcl-IV, baryte and belkovite (Blk) in dolomite carbonatite. (b) Enlarged view of U-poor Ba-rich Pcl-IV and belkovite along the radiation damaged grain margin. Note the porous nature of the Pcl-IV due to extensive metamictisation. (c, d) Association of late-formed Pcl-IV and belkovite with relict U-rich Pcl-IIa illustrating depletion in U content and subsequent Ba enrichment along the grain margin. (e) Alteration assemblage of belkovite and Pcl-IV formed after Pcl-IIa in dolomite carbonatite. Note a large baryte crystal is also present together with the belkovite. (f) Pyrochlore grain (Pcl-IIa) associated with baryte and apatite (Apt), within the dolomite matrix in banded carbonatite. (g) Alteration assemblage of baotite and an unidentified U-Nb oxide formed after U-rich Pcl-IIa along the grain margin in banded carbonatite.

**Table 3.** Representative compositions of belkovite and baotite.

Wt.%	1	2	3	4	5	6	7	8
Na <sub>2</sub> O	bdl	0.12	bdl	bdl	bdl	bdl	bdl	bdl
K <sub>2</sub> O	0.36	0.46	bdl	0.12	0.95	bdl	bdl	bdl
CaO	bdl	bdl	0.11	bdl	bdl	0.56	0.88	bdl
SrO	bdl	bdl	bdl	bdl	0.67	0.57	0.60	0.86
BaO	30.76	31.20	32.10	31.38	28.66	33.81	32.36	30.19
PbO	bdl	bdl	bdl	bdl	bdl	bdl	bdl	1.76
UO <sub>2</sub>	bdl	bdl	bdl	bdl	bdl	0.87	0.56	1.96
FeO	bdl	bdl	bdl	bdl	bdl	5.40	6.33	6.59
Al <sub>2</sub> O <sub>3</sub>	bdl	0.19	bdl	bdl	0.06	bdl	bdl	bdl
Fe <sub>2</sub> O <sub>3</sub>	1.17	1.49	2.07	1.39	1.51	bdl	bdl	bdl
TiO <sub>2</sub>	2.64	2.59	3.06	2.69	2.79	13.86	13.05	14.55
SnO <sub>2</sub>	0.32	0.61	bdl	0.67	bdl	bdl	bdl	bdl
ZrO <sub>2</sub>	bdl	bdl	bdl	bdl	1.00	bdl	bdl	bdl
Nb <sub>2</sub> O <sub>5</sub>	41.77	41.56	41.63	42.51	43.92	25.45	27.63	26.04
Ta <sub>2</sub> O <sub>5</sub>	1.53	0.88	bdl	0.83	bdl	1.09	0.41	0.99
SiO <sub>2</sub>	17.55	17.29	17.38	17.50	19.19	12.98	13.80	13.21
Cl	bdl	bdl	bdl	bdl	bdl	1.65	1.79	1.36
Total	96.10	96.39	96.35	97.09	98.75	96.24	97.41	97.51
O≡Cl	-	-	-	-	-	0.37	0.40	0.31
Sum	95.74	95.81	96.35	96.97	98.75	95.87	97.01	97.20
Apfu on the basis of 26 oxygens (belkovite) and 16 cations (baotite)								
Na	-	0.057	-	-	-	-	-	-
K	0.118	0.151	-	0.039	0.295	-	-	-
Ca	-	-	0.030	-	-	0.177	0.271	-
Sr	-	-	-	-	0.095	0.098	0.100	0.145
Ba	3.095	3.141	3.224	3.130	2.734	3.918	3.648	3.445
Pb	-	-	-	-	-	-	-	0.138
U	-	-	-	-	-	0.057	0.036	0.127
Fe <sup>2+</sup>	-	-	-	-	-	1.336	1.523	1.605
Al	-	0.058	-	-	0.017	-	-	-
Fe <sup>3+</sup>	0.226	0.288	0.399	0.266	0.307	-	-	-
Ti	0.510	0.501	0.590	0.515	0.511	3.084	2.825	3.187
Sn	0.033	0.062	-	0.068	-	-	-	-
Zr	-	-	-	-	0.119	-	-	-
Nb	4.848	4.828	4.823	4.892	4.834	3.403	3.594	3.428
Ta	0.107	0.061	-	0.057	-	0.088	0.032	0.078
Si	4.506	4.443	4.455	4.455	4.673	3.839	3.971	3.847
Cl	-	-	-	-	-	0.827	0.873	0.671

1-5: belkovite (dolomite carbonatite); 1-4: this work; 5: Voloshin *et al.*, 1990; 6-9: baotite (banded carbonatite)  
 All compositions were analysed by ED X-ray spectrometry (Lakehead University)  
 bdl: below detection limit  
 All Fe is calculated as Fe<sup>3+</sup> for belkovite and Fe<sup>2+</sup> for baotite

(1977) and the IMA pyrochlore nomenclature (Atencio *et al.*, 2010) (Table 4).

At Sevattur all Pb-rich Pcl-I are plumbopyrochlore or oxyplumbopyrochlore (Table 4). Regardless of the high U content in Pcl-II and Pcl-III, it is disappointing to note that the IMA nomenclature results in classification of the majority of these either as oxycalcipyrochlore or kenopyrochlore/hydroxyrochlore (Table 4). This nomenclature results in a consequent loss of valuable petrogenetic information. In contrast, following the (Hogarth, 1977) nomenclature these pyrochlore are classified as uranpyrochlore, a name which illustrates their major compositional characteristics and permits comparisons with previous investigations of pyrochlore in carbonatites.

In general, the majority of the U-, Ba-, Sr-rich pyrochlore have significant A- and Y-site vacancies. This is a common feature of pyrochlore and an increase in cation deficiencies at the A-site is typically associated with the progressive alteration together with introduction of large cations such as Ba, Sr and K. (Lumpkin and Ewing, 1995, 1996; Wall *et al.*, 1996; Nasraoui and Bilal,

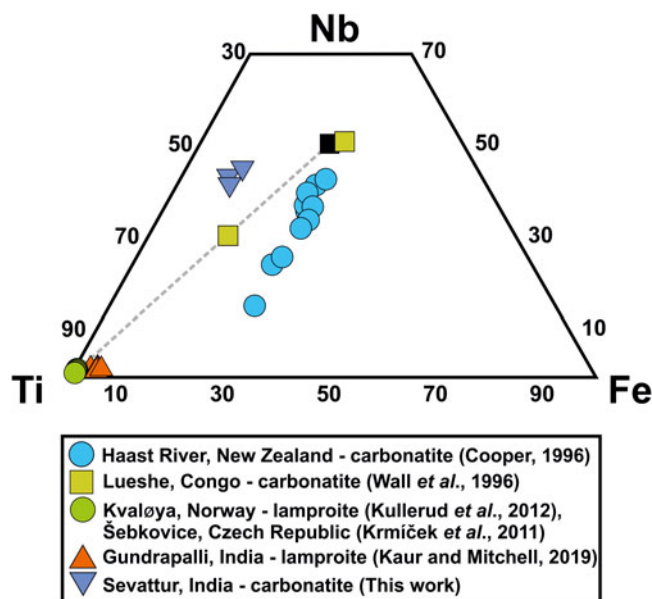


**Fig. 6.** Ti-Nb-Fe (apfu%) ternary diagram showing the relatively Nb-Ti-rich nature of Sevattur baotite. Data for some other occurrences of baotite from different lithologies are shown for comparison. Note that the only reported occurrence of baotite from the Gundrapalli lamproite, India is essentially Ti-rich. Ideal end-members (Nb- and Ti-rich, respectively) are marked in black squares, and are connected by a dotted line.

2000; Zurevinski and Mitchell, 2004). In the Hogarth (1977) nomenclature compositional names such as bariopyrochlore, strontipyrochlore, plumbopyrochlore and uranpyrochlore can be used to indicate changes in the melt/fluid composition or the process(es) that led to the enrichment of these elements in pyrochlore. Unfortunately, in IMA nomenclature all of these pyrochlore are grouped into a single species zero-valence-dominant pyrochlore, regardless of the U, Ba and Sr content at the A-site (Atencio *et al.*, 2010; Christy and Atencio, 2013).

At Sevattur, one Ba-rich Pcl-IV (Table 2, comp. 11) can be classified as oxybariopyrochlore (Ba<sub>2</sub>Nb<sub>2</sub>O<sub>7</sub>), this is probably a new species of the pyrochlore group with Ba as the dominant A-site cation (Table 4). All other Pcl-IV can be termed kenopyrochlore/hydroxyrochlore, kenobariopyrochlore/hydrobariopyrochlore (either of them could be a new species), and hydroxykenopyrochlore/hydroxyrochlore. Some Pcl-IV can be classified as uranpyrochlore or bariopyrochlore (Table 2; compositions 11-15) depending on the relative abundance of Ba and U contents (apfu) following Hogarth (1977). All the Pcl-V are Si-rich pyrochlore for which no IMA name exists (Table 4).

In terms of end-member composition, both nomenclatures commonly fail to define a unique end-member formula corresponding to a particular pyrochlore species. However, in a few instances following the dominant-valency rule together with double occupancy at a single site e.g. the A-site, charge-balanced end-members such as fluornatropyrochlore (NaCaNb<sub>2</sub>O<sub>6</sub>F), oxycalcipyrochlore (Ca<sub>2</sub>Nb<sub>2</sub>O<sub>7</sub>), or oxyplumbopyrochlore (Pb<sub>2</sub>Nb<sub>2</sub>O<sub>7</sub>) are possible. Problems arise with multiple heterovalent substitutions (including vacancies) which are more prevalent at the A-site and the dominant-valency rule typically fails to yield a charge-balanced end-member (Bosi *et al.*, 2019a), such as kenopyrochlore/hydroxyrochlore (□<sub>2</sub>Nb<sub>2</sub>O<sub>6</sub>□)<sup>22-</sup> (Table 2;

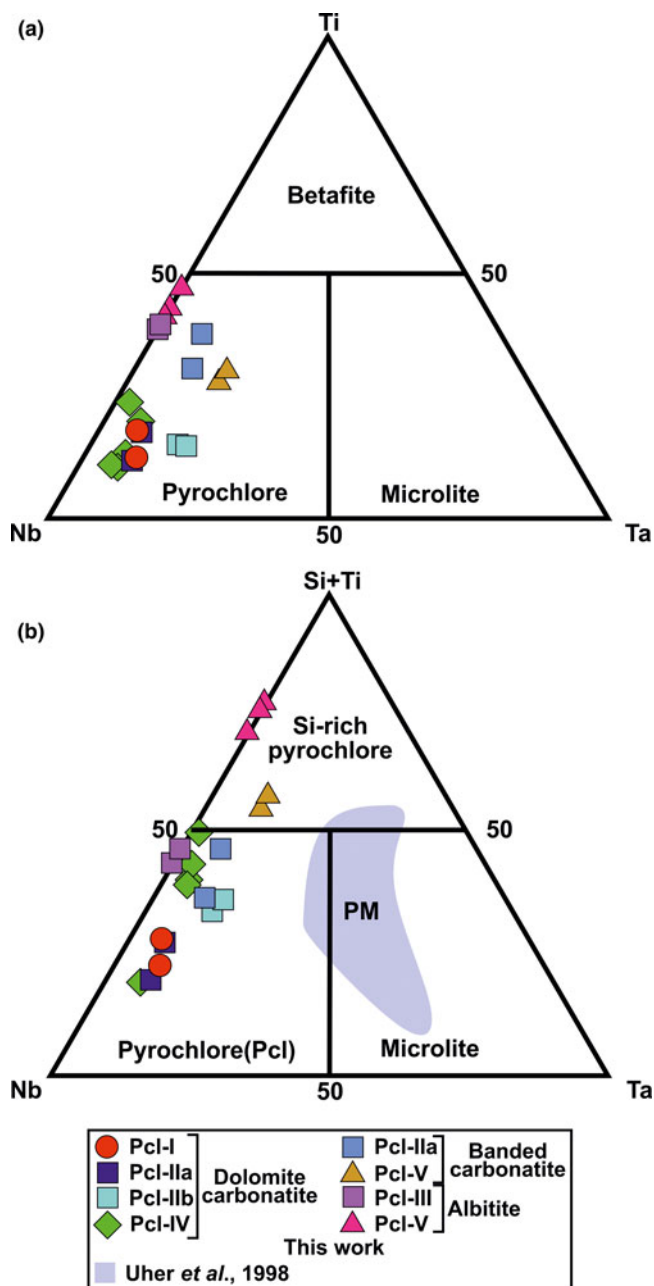


**Fig. 7.** (a) Compositional variation of the *B*-site cations (apfu) of different pyrochlore types from the Sevattur carbonatite complex. (b) Ternary plot of Nb–Ta–(Si + Ti) (apfu) illustrating the progressive Si enrichment from early- to late-generation pyrochlore. Si-rich pyrochlore plot in the (Si + Ti) field. Similar Si enrichment is seen at the Prašivá massif (PM), Slovakia. Note that the Pcl-V in banded carbonatite and albite are extremely Si-rich and comparable with some of the Prašivá massif pyrochlores.

composition 14). This problem is addressed in the recent IMA classification (Atencio *et al.*, 2010) by introducing a sub-ordinate charge-balancing component, with the end-member formula re-written as  $(\square, \#)_2\text{Nb}_2\text{O}_6\square$ , where ‘#’ could be Ba or  $\text{U}^{4+}$ .

In such cases, the application of the ‘Site Total Charge’ (STC) method is useful. Here the total charge of a site is calculated and expressed in whole numbers and the most abundant atomic arrangement (complementing the site charge) is given end-member status (Bosi *et al.*, 2019a, b). Thus, the end-member formula using STC for the above composition is

$(\square_{1.25}\text{U}_{0.75})\text{Nb}_2\text{O}_6\text{OH}$  (with  $\text{OH}^-$  used for charge balancing) resulting in the species name hydroxykenopyrochlore/hydroxyhydroxydrochlore (Table 4; serial number 14) (Supplementary material 1; serial number 14). We also suggest usage of appropriate adjectival modifiers (see Bayliss *et al.*, 2005) to represent the major cations at the *A*-site, not reflected in the IMA species name, as Ba-bearing, U-rich hydroxykenopyrochlore/hydroxyhydroxydrochlore, where  $\text{U}^{4+}$  is the dominant cation (0.5 apfu) and there is also a considerable amount of Ba (0.3 apfu) at the *A*-site (Table 2; composition 14) (for calculation of end-member formula of all pyrochlore species from Sevattur using the STC method; see Supplementary material 1). This method is helpful in understanding the compositional diversity that exists among the pyrochlore-group minerals and certainly a more useful representation than the IMA scheme, especially for practical petrogenetic aspects associated with pyrochlore compositions and their evolution.

#### Belkovite and baotite

Sevattur belkovite can be represented by an empirical formula of  $^A(\text{Ba}_{3.10}\text{K}_{0.12})_{\Sigma 3.22}^B(\text{Nb}_{4.85}^{5+}\text{Ta}_{0.11}^{5+}\text{Ti}_{0.51}^{4+}\text{Sn}_{0.03}^{4+}\text{Fe}_{0.23}^{3+})_{\Sigma 5.73}^X\text{Si}_{4.51}^Y\text{O}_{26}$  (Table 3; composition 1) based on 26 oxygens. Simple application of the dominant-valency rule, to the above empirical formula leads to an end-member composition of  $\text{Ba}_3\text{Nb}_6\text{Si}_4\text{O}_{26}$ , which is close to a synthetic barium silicon tantalum oxide ( $\text{Ba}_3\text{Ta}_6\text{Si}_4\text{O}_{26}$ ) (Choisnet *et al.*, 1976). However, there is excess of total cations (13.45), which can be justified by the fact that the structure of  $\text{Ba}_3\text{Ta}_6\text{Si}_4\text{O}_{26}$  has two sites for larger cations, at  $(x, 0, 1/2)$  and  $(x, 0, 0)$  respectively. When the larger cation is  $\text{Ba}^{2+}$  the latter site is empty, when the larger cation is  $\text{K}^+$  it is fully occupied, giving a total of 16 cations, as in the synthetic compound  $\text{K}_6\text{Nb}_6\text{Si}_4\text{O}_{26}$  (Choisnet *et al.*, 1976). So, it can be argued that the structure of belkovite is able to accommodate >13 cations. But, the presence of excess of Si (>4 apfu) cannot be justified as Si is supposed to be restricted to the tetrahedral *X* site. Therefore, excess Si could be an analytical error leading to silica ( $\text{SiO}_2$ ) over-estimation. To eliminate the excess silica, the belkovite formula can also be calculated on the basis of 4 Si cations. However, this results in significantly low total oxygens (~23 apfu), which can only be balanced by considering the presence  $\text{OH}^-$  along with oxygen at the *Y* site. Moreover, the presence of  $\text{OH}^-$  could be a possibility reflected in low analytical totals, and recalculated  $\text{H}_2\text{O}$  (wt.%) obtained by this method makes the analytical total close to one hundred. However, lack of structural data refrains us from assuming the presence of water in belkovite. This suggests a further investigation on the crystallo-chemical aspects of belkovite is needed.

The site-total-charge approach suggests  $(\text{Nb}_4^{5+}\text{Ti}_2^{4+})_{\Sigma 28}^{28+}$  as the most abundant charge arrangement at the *B*-site. Thus, the end-member formula for belkovites from the Sevattur can be written as  $\text{Ba}_3(\text{Nb}_4\text{Ti}_2)\text{Si}_4\text{O}_{25}$  (see Supplementary Material 2).

Baotite end-member compositions vary between  $\text{Ba}_4\text{Ti}_8\text{Si}_4\text{O}_{28}\text{Cl}$  and  $\text{Ba}_4\text{Ti}_2\text{Nb}_4\text{Fe}_2\text{Si}_4\text{O}_{28}\text{Cl}$  (Krmíček *et al.*, 2011; Kullerud *et al.*, 2012; Kaur and Mitchell, 2019 and references therein). The role of chlorine in the baotite structure is enigmatic, commonly it is considered as a neutral species and not required to balance the structure electrostatically (Nekrasov *et al.*, 1969; Nemeč, 1987; Potter and Mitchell, 2005; Kullerud *et al.*, 2012). However, following the STC method, baotites from Sevattur have an ideal composition of  $\text{Ba}_4\text{Ti}_3(\text{Nb}_{3.33}\text{Fe}_{1.67})\text{Si}_4\text{O}_{28}\text{Cl}_n$ , where *n* varies from 0.7 to 0.9 (see Supplementary material 2).



**Table 4.** Classification and end-member formula of pyrochlore-group minerals from Sevattur.

Serial No.	End-member formula	Hogarth (1977)	Atencio <i>et al.</i> (2010)	Adjectival modifiers
1	#Pb <sub>2</sub> Nb <sub>2</sub> O <sub>6</sub> O	plumbopyrochlore	oxyplumbopyrochlore	U-bearing
2	#Pb <sub>2</sub> Nb <sub>2</sub> O <sub>6</sub> O	plumbopyrochlore	oxyplumbopyrochlore	U-bearing
3	#Ca <sub>2</sub> Nb <sub>2</sub> O <sub>6</sub> O	uranpyrochlore	oxycalcipyrochlore	U-bearing
4	#Ca <sub>2</sub> Nb <sub>2</sub> O <sub>6</sub> O	uranpyrochlore	oxycalcipyrochlore	U-bearing
5	*([ <sub>1.5</sub> U <sub>0.5</sub> )Nb <sub>2</sub> O <sub>6</sub> □	uranpyrochlore	kenopyrochlore/hydropyrochlore	U-rich
6	#Ca <sub>2</sub> Nb <sub>2</sub> O <sub>6</sub> O	uranpyrochlore	oxycalcipyrochlore	U-rich
7	#Ca <sub>2</sub> Nb <sub>2</sub> O <sub>6</sub> O	uranpyrochlore	oxycalcipyrochlore	U-bearing
8	*(Ca□)Nb <sub>2</sub> O <sub>6</sub> □	pyrochlore	kenocalcipyrochlore/hydrocalcipyrochlore	Ba-bearing
9	#Ca <sub>2</sub> Nb <sub>2</sub> O <sub>6</sub> O	uranpyrochlore	oxycalcipyrochlore	U-bearing
10	*([ <sub>1.5</sub> U <sub>0.5</sub> )Nb <sub>2</sub> O <sub>6</sub> □	uranpyrochlore	kenopyrochlore/hydropyrochlore	U-rich
11	#Ba <sub>2</sub> Nb <sub>2</sub> O <sub>6</sub> O	uranpyrochlore	<sup>§</sup> oxybariopyrochlore	U-rich
12	*(□Ba)Nb <sub>2</sub> O <sub>6</sub> □	bariopyrochlore	kenopyrochlore/hydropyrochlore	U-bearing
13	*(Ba□)Nb <sub>2</sub> O <sub>6</sub> □	bariopyrochlore	<sup>§</sup> kenobariopyrochlore/hydrobariopyrochlore	-
14	*([ <sub>1.25</sub> U <sub>0.75</sub> )Nb <sub>2</sub> O <sub>6</sub> OH	uranpyrochlore	hydroxykenopyrochlore/hydroxyhydropyrochlore	Ba-bearing, U-rich
15	*(□Ba)Nb <sub>2</sub> O <sub>6</sub> □	bariopyrochlore	kenopyrochlore/hydropyrochlore	Ba-rich
16	*(□Ca)Nb <sub>2</sub> O <sub>6</sub> □	betafite	kenopyrochlore/hydropyrochlore	Ca-rich
17	*(□) <sub>2</sub> Nb <sub>2</sub> (O <sub>4</sub> OH <sub>2</sub> )□	betafite	kenopyrochlore/hydropyrochlore	Ca-rich
18	<sup>§</sup> Ca <sub>2</sub> Si <sub>2</sub> O <sub>6</sub> □	betafite	<sup>§</sup> unnamed	Ca-rich
19	*(□Ca)Nb <sub>2</sub> O <sub>6</sub> □	pyrochlore	kenopyrochlore/hydropyrochlore	Ca-rich
20	*(□Ca)Nb <sub>2</sub> O <sub>6</sub> □	uranpyrochlore	kenopyrochlore/hydropyrochlore	Ca-rich

1–2: Pcl-I; 3–6: Pcl-IIa; 7–8: Pcl-IIb; 9–10: Pcl-III; 11–15: Pcl-IV; 16–20: Pcl-V; #end-member formula in accordance with the dominant-valency rule; \*end-member formula calculated by the STC method (Bosi *et al.*, 2019a, b); <sup>§</sup>possible news species; <sup>§</sup>end-member formula with Si-dominant at the B-site (Ca<sub>2</sub>Si<sub>2</sub>O<sub>6</sub>□) is not possible so is discredited; unnamed: no group name exists at present, having Si<sup>4+</sup> as the dominant cation of the dominant valency at the B-site.

## Discussion

### Pyrochlore substitutional mechanisms, alteration and related compositional variation

Pyrochlore-group minerals at Sevattur show wide compositional variations. These diverse compositions are useful for discerning the diverse magmatic and post-magmatic processes which led to their formation. In general, U-rich pyrochlores are characterised by extensive metamictisation and damaged crystal structures making them susceptible to moderate-to-intense alteration and U mobility (Lumpkin and Ewing, 1995, 1996; Hogarth *et al.*, 2000). Intense alteration of such pyrochlores leads to patchy zoning characterised by several high-AZ, intermediate-AZ, and low-AZ zones as evident in BSE images (Figs 3, 5). Compositionally, these pyrochlores are extremely heterogeneous and therefore no single trend of evolution is evident. Sevattur pyrochlores show a gradual change in composition from U-rich pyrochlore (Pcl-II, -III) to Si-rich pyrochlore (Pcl-V) through Ba-Si-rich pyrochlore (Pcl-IV) with a variable Ta/Ti ratios. A systematic increase in Si and Ba at the expense of Nb from Pcl-I to Pcl-IV (dolomite carbonatite) and Pcl-IIa to Pcl-V (banded carbonatite and albitite) can be explained by the following coupled substitution:



involving both the A- and B-sites with a negative correlation ( $R = -0.89$  and  $-0.97$ ) (Fig. 8a,b). The Ba enrichment reaches a maximum in the dolomite carbonatite. Ba-rich pyrochlore is typically considered to form during late-stage hydrothermal or supergene alteration (Jager *et al.*, 1959; Harris, 1965; Traversa *et al.*, 2001; Melgarejo *et al.*, 2012). Although, primary Ba-pyrochlore with >11 wt.% BaO has been reported from Araxá (Brazil), this was subsequently replaced along fractures by a later generation of Ba-rich pyrochlore (Mitchell, 2015). At Sevattur, the enrichment of Ba coupled with an increase in

A-site vacancy at the expense of Ca is prominent for Pcl-IV (Fig. 8c) and reflects the following substitution with a negative correlation ( $R = -0.93$ ):



The compositional variation of Pcl-IV is the result of extensive metamictisation and development of numerous cracks/fractures which facilitate U mobility with concomitant increase in Ba. The Nb depletion with increasing Si can be explained by a Nb *versus* Si substitution, which in a bivariate plot shows an excellent correlation for the carbonatites (dolomite and banded;  $R = -0.93$ ) and albitite ( $R = -0.96$ ) (Fig. 8d,e) respectively. This correlation is also evident for other occurrences of Si-rich pyrochlore (Fig. 8f).

Lumpkin and Ewing (1995; 1996) have defined three different alteration trends: primary; transitional; and secondary, to represent the compositional variation in pyrochlore-group minerals during progressive alteration. Sevattur pyrochlore are characterised by low Na contents and loss of U and Ca, coupled with increase in Ba- and A-site vacancies from early (Pcl-I, -IIa and -III) to late (Pcl-IIb, -IV and -V) pyrochlore generations as shown in Figs 9a and b. Three broad trends are shown in the  $A^{4+}-A^{2+}-A$ -vacancy plot (Fig. 9a): (1) increase in A-site vacancies with near-constant values of U<sup>4+</sup> from Pcl-I to U-rich Pcl-III (Trend 1); (2) depletion of U<sup>4+</sup> with near-constant A-site vacancies in Pcl-IV (from U-rich to U-poor) (Trend 2); and (3) a further increase in A-site vacancies at low U content (Trend 3) in some Pcl-IV and Pcl-V. The compositional variation of Pcl-IV is significantly different compared to that of other pyrochlores (Fig. 9a) and is due mainly to the variation in U and Ba contents. The initial alteration of Pcl-IV resulted in the substantial loss of U at constant Ca (Fig. 8c; Supplementary material 3; HA1–HA4) without significant Ba-enrichment. Although, for some Pcl-IV the effect of Ba, Si-enrichment is more conspicuous with a variable degree of U loss (Fig. 9a; Table 2; compositions 11–15).

Simple correlations between U, Ca, Ba and Si are difficult to establish.

It is evident that all the pyrochlores from the carbonatites have exceptionally low contents of monovalent cations and show a gradual increase in *A*-site vacancies during evolution from Pcl-I to Pcl-V (Fig. 9b). However, the Si-rich Pcl-V and Pcl-III in albitite are distinctly different from those occurring in carbonatite being enriched in Na and K (Fig. 9b).

### Uranium and niobium mobilisation in pyrochlore

Uranium-rich pyrochlore might have diverse origins and can be a primary magmatic phase or crystallise subsequently to Na-Ca pyrochlore (Mitchell, 2015). Uranium is soluble as fluorides and sulfates at low pH (acidic); as phosphates at neutral pH; and as carbonates and hydroxides in alkaline conditions (Boyle, 1982). Experimental studies have shown that a hot, acidic, chloride-rich solution is capable of transporting  $U^{4+}$  as a uranium chloride species ( $UCl_4^0$ ) under reducing conditions (Geisler *et al.*, 2004; Migdisov *et al.*, 2018; Timofeev *et al.*, 2018).

Considering the overall mineral assemblages present at the Sevattur carbonatite complex (Table 1),  $CO_3^{2-}$ ,  $SO_4^{2-}$ ,  $F^-$ , and  $Cl^-$  are the primary ligands which are capable of mobilising uranium during alteration of U-rich pyrochlore. This hypothesis is supported by the ubiquitous presence of baryte and different carbonates (dolomite and calcite) in association with Pcl-IIa, Pcl-IIb and Pcl-IV, and suggests that  $CO_3^{2-}$  and  $SO_4^{2-}$  played an important role in mobilising uranium as uranyl complexes in dolomite carbonatite (Fig. 5a–e). In contrast, the banded carbonatite with an assemblage of baotite, U-rich Pcl-IIa and baryte suggests that  $CO_3^{2-}$ ,  $SO_4^{2-}$ , and  $Cl^-$  facilitated the uranium mobilisation resulting in the formation of an exceptionally uranium-rich phase (>63 wt.%  $UO_2$ ) (Fig. 5f,g). The formation of baotite and the unknown U-rich phase with relict unaltered U-rich Pcl-IIa probably suggests that the uranium mobilisation might have taken place by the interaction with a  $Cl^-$ -rich hot acidic solution under alkaline and reducing conditions at least on a micrometre scale.

Albitite-hosted pyrochlores (Dey *et al.*, 2021) are the most U-rich (Pcl-III; >36 wt.%  $UO_2$ ) and the majority of these are enveloped by a Ba-rich potassium feldspar mantle (Fig. 3d). However, there are pyrochlores that either lack mantles or these are partially disrupted (Fig. 3h), resulting in the formation of Si-rich and U-poor pyrochlore (Pcl-V) as evidenced by the strong correlation of the *B*-site cations (Nb, Ta and Ti) versus Si (Fig. 8d). Thus, the formation of Pcl-V in albitite took place upon interaction with a late-stage Ba-Si-rich aqueous fluid. These features suggest that the Ba-rich potassium feldspar mantle around Pcl-III, restricted U-mobility compared to the pyrochlores in the carbonatites.

In the pyrochlore structure, *B*-site cations (Nb, Ta and Ti) are relatively immobile and remain unaffected by hydrothermal alteration and weathering processes (Lumpkin and Ewing, 1995). Although the late-stage alteration of pyrochlore shows that at temperature <150°C niobium is remobilised by diffusion from  $BO_6$  octahedra (Lumpkin and Ewing 1995, Geisler *et al.*, 2004). Experimental studies have shown that the mobilisation of *B*-site cations is possible in acidic fluoride-rich hydrothermal solutions. Increasing HF activity in the fluid makes Nb more soluble than Ta regardless of the temperature (Timofeev *et al.*, 2015; 2017; Akinfiev *et al.*, 2020). Consequently, the removal of HF from the hydrothermal solution by precipitation of fluorite and

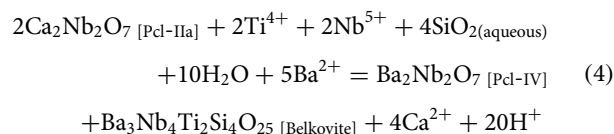
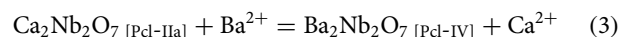
fluorapatite could enhance Nb-mineral precipitation (Timofeev *et al.*, 2015; 2017). Even under low-temperature, alkaline conditions (pH > 8), Nb leaching and transportation are possible as polyoxometalate Lindqvist ions [ $(H_xNb_6O_{19})^{(8-x)-}$ ] which implies that surficial weathering processes are quite effective in mobilising Nb as polyoxometalate ions (Friis and Casey, 2018).

In common with uranium, mobility of Nb is also observed during alteration of Pcl-IIa to Pcl-IIb in dolomite carbonatite, and Pcl-III to Pcl-V in albitite (Fig. 4a; Table 2). In dolomite carbonatite, the association of Pcl-IIa together with Pcl-IV and secondary minerals such as baryte and belkovite suggest that Nb was liberated from the pyrochlore upon interaction with a sulfate-rich solution. The alteration sequence of U-rich pyrochlore to belkovite in the dolomite carbonatite through an intermediate metamict pyrochlore (Pcl-IV) with low analytical totals (~76–86 wt.%) (Supplementary material 3) suggests that the Nb mobilisation was accompanied by Ba, and Si enrichment. The formation of baotite in the banded carbonatite suggests that Nb mobilisation was accompanied by Ba, Ti and Si enrichment in the presence of  $Cl^-$  during the alteration process. Furthermore, late-stage Ba, Si enrichment resulted in the formation of Si-rich Pcl-V and baryte. Considering the very low modal abundance of baotite relative to baryte; it is probable that baryte was formed late in the paragenetic sequence. In contrast to the carbonatites, albitite also shows significant Nb mobilisation during alteration from U-rich Pcl-III to Si-rich Pcl-V. The absence of apatite or fluorite in albitite probably suggests that the Nb mobilisation might have been triggered by the sulfate-bearing solutions alone.

### Genesis of pyrochlore, belkovite and baotite

Sevattur pyrochlore-group minerals exhibit a wide compositional variation similar to those in many carbonatite complexes, e.g. St. Honoré, Prairie Lake, Oka. This could be related to the multiple episodes of carbonatitic magmatism or due to the interactions with hydrothermal fluids. Considering the complex nature of both inter- and intra-grain compositional variation within a given lithological unit, it is difficult to determine a single trend of evolution for the Sevattur pyrochlores.

In dolomite carbonatite, Pcl-I is characterised by high Pb and low Ca contents, is exclusively present as inclusions in Pcl-IIa, and was probably formed from an evolved Pb-rich hydrothermal fluid. Consequently, Pcl-I are considered as unrelated to the other pyrochlore types (Pcl-II to Pcl-IV) and were probably transported to their current host (dolomite carbonatite) by a later carbonatite pulse which crystallised Pcl-IIa on Pcl-I nuclei. The U-Ta-rich Pcl-IIa are characteristic of carbonatite pyrochlore evolution and considered to be early-forming pyrochlore (Mitchell, 2015). In contrast, Pcl-IIb with significant Pb, lower U, and high Si contents relative to Pcl-IIa, suggests that the Pcl-IIb formed by alteration of both Pcl-I and Pcl-IIa. The alteration assemblage of Pcl-IV + belkovite formed after Pcl-IIa (Fig. 3c) suggests interaction with a Ba-Si-rich hydrothermal fluid by the following reactions:



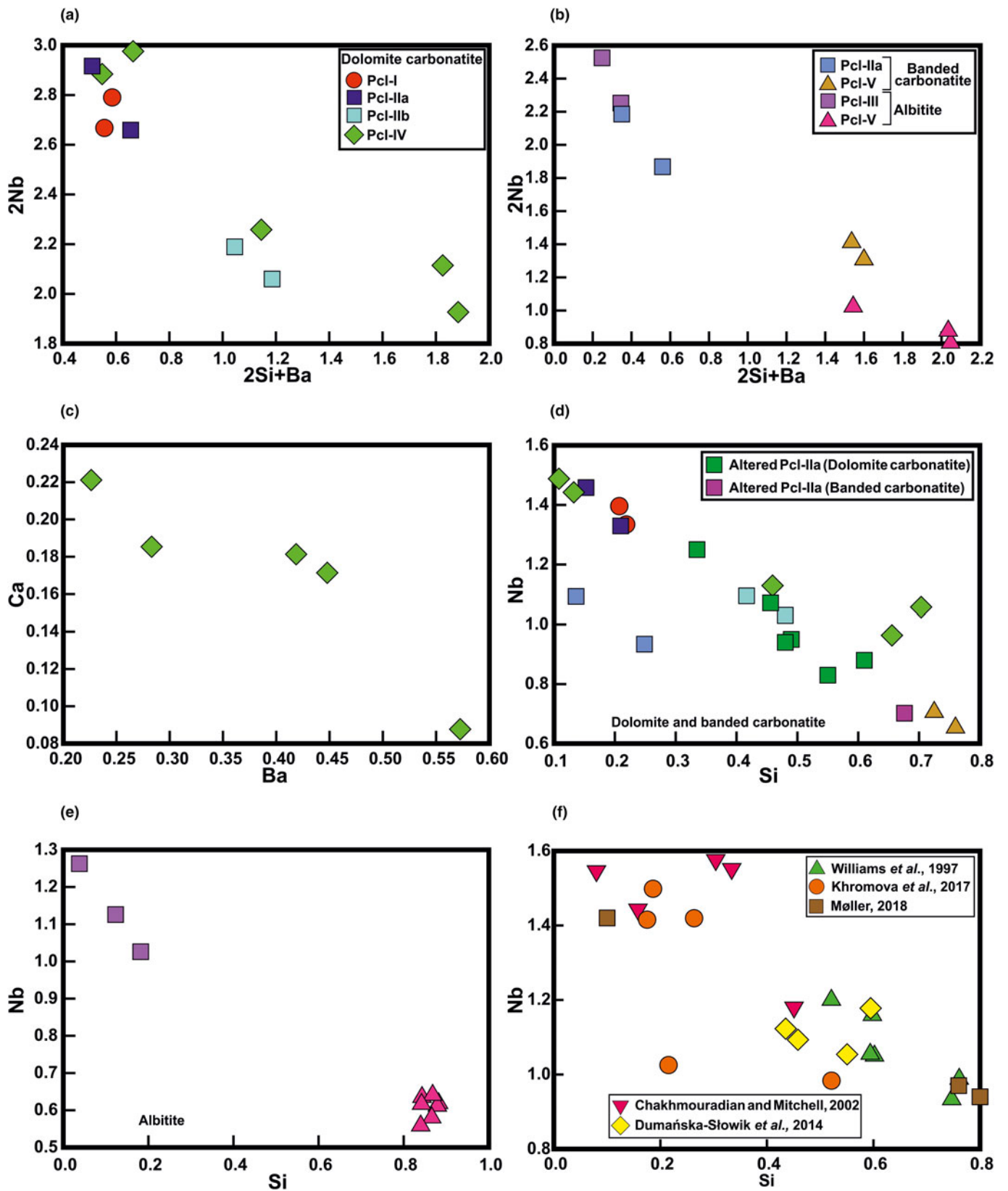


**Fig. 8.** (a,b) The  $2\text{Nb}^{5+} \rightarrow 2\text{Si}^{4+} + \text{Ba}^{2+}$  (apfu) substitution for different pyrochlore generations illustrating Ba and Si enrichment in the later generation pyrochlore (Pcl-IIb and Pcl-IV) in dolomite carbonatite. This substitution is more evident in the Pcl-V hosted by banded carbonatite and albitite. (c)  $\text{Ca}^{2+} \rightarrow \text{Ba}^{2+}$  (apfu) substitution showing Ba enrichment in Pcl-IV relative to the U-poor Ca-rich Pcl-IIa in dolomite carbonatite. (d,e) A strong negative correlation is observed in the Nb versus Si plot for all the pyrochlore generations (Pcl-I to Pcl-V) with an  $R$  value of  $-0.93$  for dolomite and banded carbonatite;  $R = -0.96$ , for albitite. (f) The figure illustrates a similar correlation for Si-rich pyrochlore from: the Bingo carbonatite, Congo (Williams et al., 1997); the Lovozero alkaline complex, Russia (Chakhmouradian and Mitchell, 2002); the Mariupol massif, Ukraine (Dumańska-Stowik et al., 2014); the Belaya Zima pluton, Russia (Khromova et al., 2017); Ímaussaq, South Greenland (Møller, 2018).



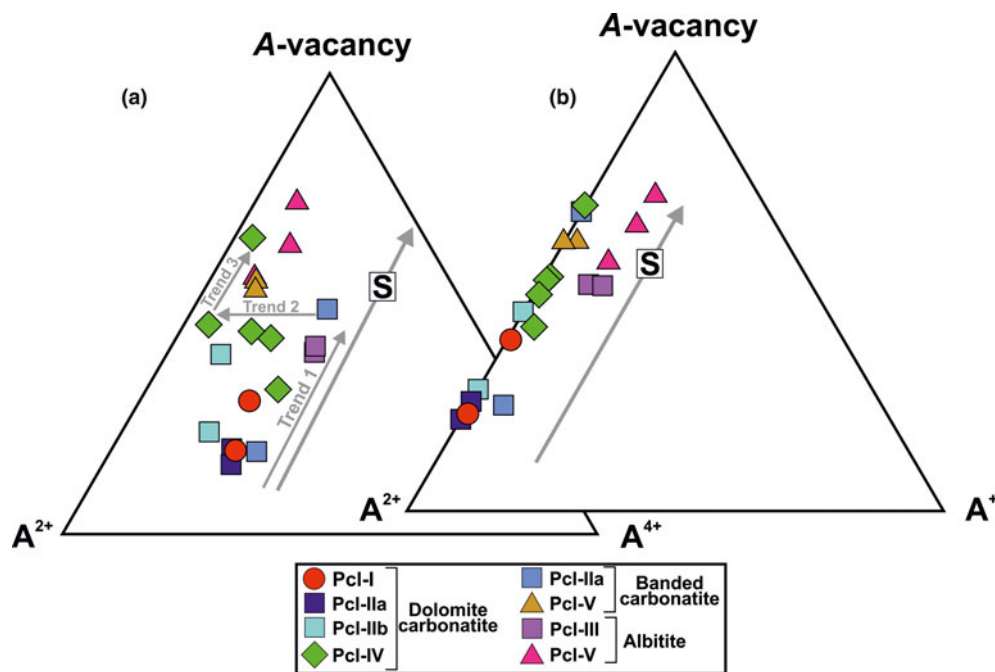
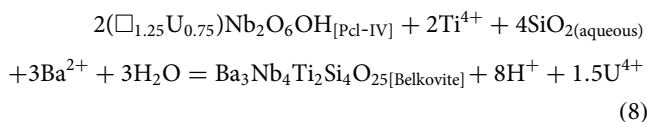
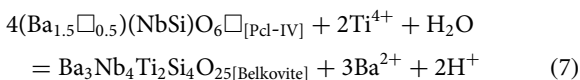
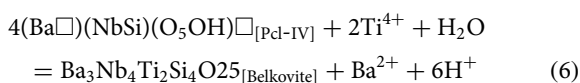
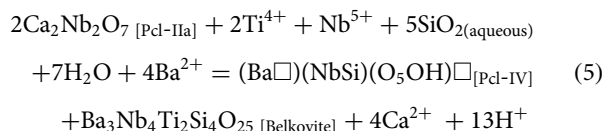


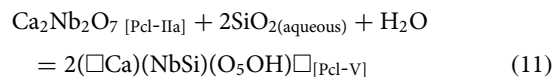
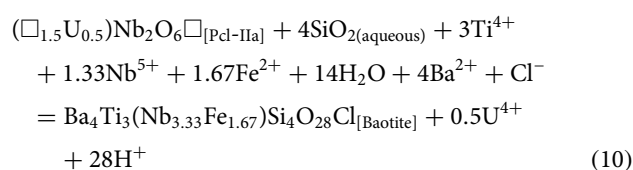
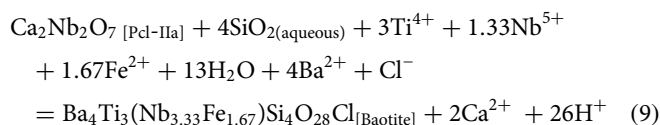
**Fig. 9.** (a) Ternary plot of  $A^{4+}$  (A-site tetravalent cations) –  $A^{2+}$  (A-site divalent cations) – A-site vacancy (apfu) (after Lumpkin and Ewing, 1995) illustrating three different trends (1, 2 and 3) related to progressive alteration from early- to late-stage pyrochlore formation (see discussion for details). Note that the significant variation in  $A^{4+}$  cations in Pcl-IV in dolomite carbonatite are related to partial replacement of Ca by Ba and subsequent loss of U. (b) Ternary plot of  $A^{2+}$ – $A^+$  (A-site monovalent cations) – A-site vacancy (apfu) (after Lumpkin and Ewing, 1995) showing the overall loss of divalent cations and subsequent increase in the A-site vacancy during progressive alteration of all pyrochlore-bearing lithologies at Sevattur. Note that the Pcl-III and Pcl-V in albitite are relatively rich in monovalent cations  $Na^+$  and  $K^+$ , respectively. Both ternary plots demonstrate the secondary (S) alteration trend of Lumpkin and Ewing (1995).



These reactions (3–7) explain the formation of Ba-Si-rich Pcl-IV and belkovite by alteration of Pcl-IIa and subsequent removal of U (reaction 8). It is worthwhile noting that belkovite is present exclusively in dolomite carbonatite and restricted to pyrochlore alteration assemblages.

In contrast, the banded carbonatite is characterised by an alteration assemblage of Si-rich Pcl-V + baotite  $\pm$  U-Nb-rich phase formed after Pcl-IIa. The formation of baotite can be explained

by the following reactions:



These reactions suggest that baotite (9, 10) and Si-rich Pcl-V (11) were formed upon interaction of Pcl-IIa with a Ba-Si-rich and a Si-rich fluid respectively. However, there are significant compositional differences in the Ba-U-Nb-Ti contents between the Pcl-IIa found in the dolomite carbonatite and banded carbonatite, respectively. Consequently, the alteration assemblages are essentially controlled by the primary composition of the pyrochlore (Pcl-IIa). The formation of baotite in the banded carbonatite results mainly from the high Ti content of Pcl-IIa compared to that in the dolomite carbonatite. The high Nb content in Pcl-IIa facilitated belkovite formation in the dolomite carbonatite. This confirms that the pyrochlore-group minerals in the different

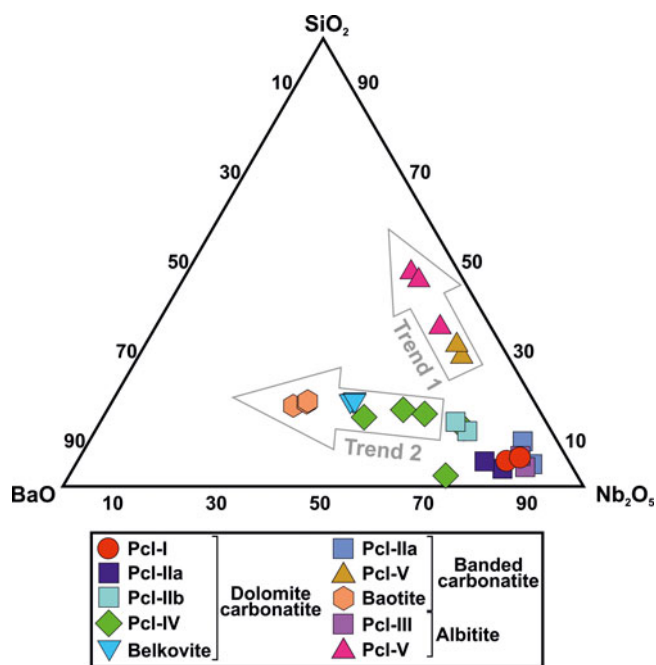
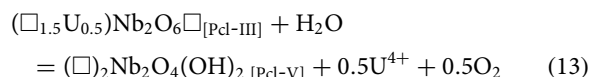


**Fig. 10.** Ternary plot of major oxides (Nb<sub>2</sub>O<sub>5</sub>-BaO-SiO<sub>2</sub>) (wt.%) for pyrochlore, belkovite and baotite showing two different trends. Trend 1 shows an extreme Si-enrichment that led to the formation of Si-rich Pcl-V. Trend 2 illustrates a progressive Ba-enrichment in Ba-rich Pcl-IV, belkovite and baotite within different Sevattur lithologies.

varieties of carbonatite are not linked genetically by differentiation and probably there is no single trend of evolution for Sevattur pyrochlores.

In albitite, U-Ti-rich Pcl-III were protected initially by the Ba-K-rich potassium feldspar mantle, but subsequently altered to Si-rich Pcl-V with significant remobilisation of U and Nb, where the mantle is disrupted. The formation of Pcl-V in albitite can be explained by the following reactions:



Note that the Si-enrichment in albitite-hosted Pcl-V can be best represented by the non-ideal end-member [(□Ca)Si<sub>2</sub>(O<sub>4</sub>OH<sub>2</sub>)□] obtained by the STC method (Supplementary material 1; serial number 16–18). As mentioned above, establishment of such an end-member formula where Si is the dominant B-site cation is not possible at present due to lack of clarity on the crystal-chemical role of Si in the pyrochlore structure.

At Sevattur, the most important feature of the pyrochlore is the lithology specific variation in composition and their unique alteration assemblages. Belkovite and baotite in dolomite and banded carbonatites are restricted exclusively to pyrochlore alteration assemblages. This lithology specific alteration assemblage

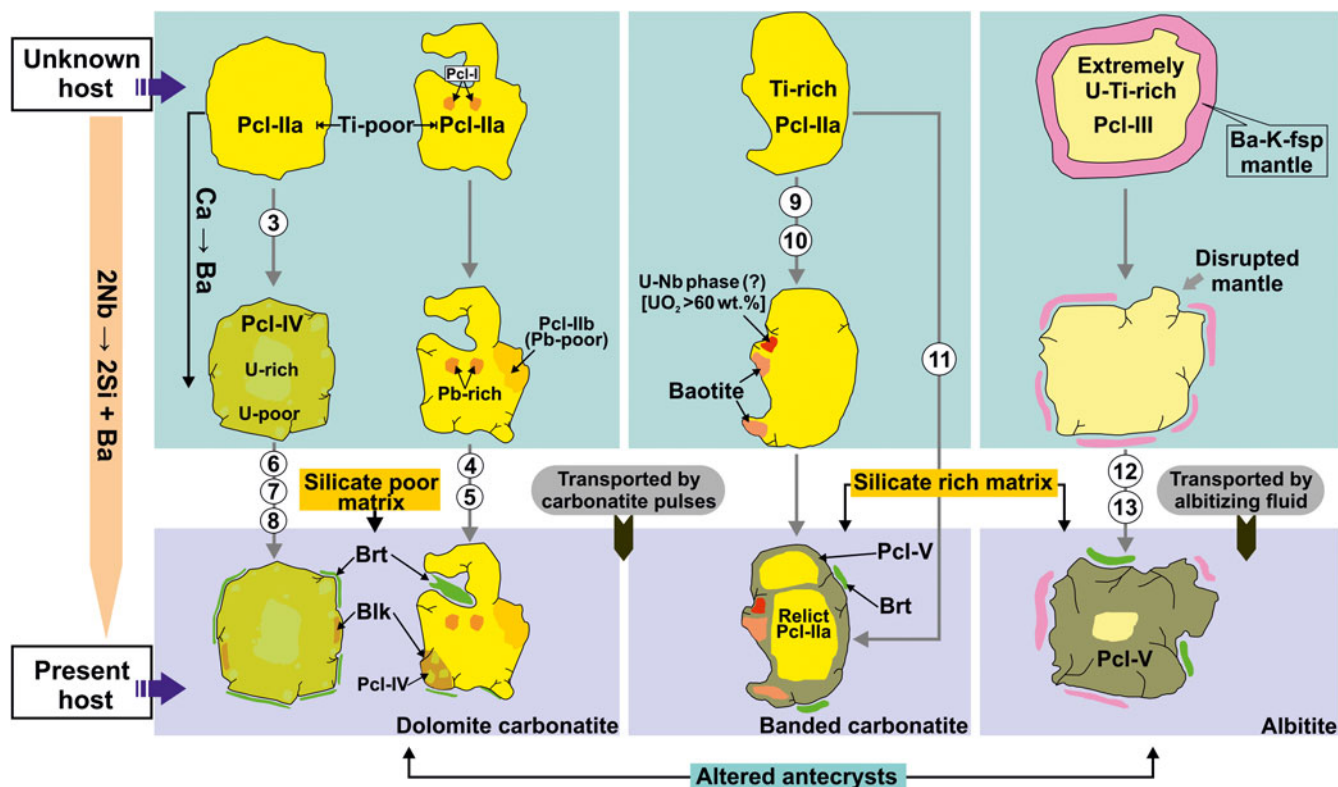


**Fig. 11.** Schematic diagram illustrating the lithology specific compositional evolution of pyrochlore and their alteration assemblages. The initial stage is the formation of early pyrochlore generations and their alteration assemblages in their respective source lithologies (unknown host). In the later stages, all the pyrochlore with their alteration assemblages were transported to their present host lithologies as altered antecrysts. Interaction with a late-stage Ba-Si-rich fluid produces Si-rich Pcl-V in banded carbonatite and albitite. Baryte (Brt) is present in all the Sevattur lithologies. Numbers marked in Arabic numerals indicate possible reaction(s) of formation of the individual pyrochlore species and related alteration assemblage(s). (see text for discussion).

indicates a very complex evolution for these pyrochlores and suggests that all have undergone several stages of alteration leading to formation of belkovite/baotite in an unknown host prior to their incorporation to the current host as altered antecrysts (a hypothesis also proposed for albitite-hosted pyrochlores at Sevattur; Dey et al., 2021). Therefore, they exhibit different styles of alteration and also different alteration assemblages, regardless of lithology (Fig. 2).

The ubiquitous presence of baryte suggests that a Ba-rich fluid affected all the lithological units at Sevattur with baryte forming very late in the paragenetic sequence. This event has resulted in Ba-Si-enrichment in all the pyrochlore types and baryte precipitation within the fractures formed by metamictisation. This is evident from the complete absence of Si-rich Pcl-V in the dolomite carbonatite as this unit is devoid of silicates compared to other Sevattur lithologies. Consequently, Ba-rich and U-poor Pcl-IV and baryte dominated the alteration assemblages formed after Pcl-IIa in the dolomite carbonatite. In contrast, the banded carbonatite and albitite with higher modal abundances of silicates facilitated the supply of Si during interaction with late-stage Ba-rich fluids (probably acidic) and formation of Pcl-V. Such Si-enrichment in all the pyrochlores and related alteration assemblages is shown in the BaO–Nb<sub>2</sub>O<sub>5</sub>–SiO<sub>2</sub> ternary diagram (Fig. 10) which shows two trends: one with increasing Si content leading to the formation of Pcl-V (Trend 1) and another with both Ba and Si enrichment resulting in the formation of Pcl-IV, belkovite and baotite (Trend 2).

## Conclusion

On the basis of texture and composition, five different pyrochlores (Pcl-I to Pcl-V) are recognised at Sevattur. Relatively unaltered, early pyrochlore generations (Pcl-I, -IIa and III) have elevated U–Ca–Nb contents compared to altered late-pyrochlores (Pcl-IIb, -IV and -V) (Fig. 11). The later-formed pyrochlores are characterised by higher Ba-, Si- and A-site vacancies. The compositional variations in different pyrochlore generations (Pcl-I to Pcl-V) suggest an overall transitional to secondary alteration.

The lithology specific alteration assemblage of Pcl-IIb + belkovite + Pcl-IV and baotite + Pcl-V ± U–Nb-rich phase in the dolomite and banded carbonatite formed after Pcl-IIa is a characteristic feature at Sevattur. These lithology specific alteration assemblages are suggestive of initial alteration within their respective sources before being carried by later carbonatite pulses as altered antecrysts to the present host (Fig. 11).

The presence of baryte in all Sevattur lithologies suggests that baryte formed late in the paragenetic sequence compared to the Pcl-I to Pcl-IV (Fig. 11). The association of baryte and Pcl-V in the banded carbonatite and albitite suggests that all the Sevattur rocks were affected by a late-stage Ba-rich acidic hydrothermal fluid. This fluid scavenged silica from the associated silicates to an extent dependent upon their relative modal abundances. This observation is in accordance with the presence of Si-rich Pcl-V in albitite and banded carbonatite as a consequence of the high modal abundance of silicate phases. This conclusion is further substantiated by the complete absence of Pcl-V in the dolomite carbonatite, which has a very low modal abundance of silicates (Fig. 11). Thus, the compositional diversity of pyrochlore-group minerals at Sevattur is complex and related to the superposition of multiple events spanning from magmatic to hydrothermal processes.

**Acknowledgements.** This work is supported by the Ministry of Mines (MOM), India, through an Extra Mural Project (F.No. 8/4/2009-Met.IV Dt. 27.11.2014) awarded to AKS and AC. MD, SB and AC also acknowledge Prof. K. N. Ganesh, Director, IISER Tirupati for providing financial assistance through an Institute Travel Grant to carry out necessary field work. R. H. Mitchell's work on alkaline rocks is supported by the Natural Sciences and Engineering Research Council of Canada, Lakehead University and Almaz Petrology Inc. We are thankful to Ferdinando Bosi and Kåre Kullerud for extending their help to understand the intricacies of the STC method and baotite structure. We acknowledge Jan Cempírek and an anonymous reviewer for their valuable suggestions which helped to improve the manuscript significantly. We acknowledge Stuart Mills and Helen Kerbey for the Editorial and production aspects of the publication of this work.

**Supplementary material.** To view supplementary material for this article, please visit <https://doi.org/10.1180/mgm.2021.37>

## References

- Ackerman L., Magna T., Rappich V., Upadhyay D., Krátký O., Čejková B., Erban V., Kochergina Y.V. and Hrstka T. (2017) Contrasting petrogenesis of spatially related carbonatites from Samalpatti and Sevattur, Tamil Nadu, India. *Lithos*, **284**, 257–275.
- Akinfiyev N.N., Korzhinskaya V.S., Kotova N.P., Redkin A.F. and Zotov A.V. (2020) Niobium and tantalum in hydrothermal fluids: Thermodynamic description of hydroxide and hydroxofluoride complexes. *Geochimica et Cosmochimica Acta*, **280**, 102–115.
- Andersen T. (1986) Magmatic fluids in the Fen carbonatite complex, SE Norway. *Contributions to Mineralogy and Petrology*, **93**, 491–503.
- Atencio D., Andrade M.B., Christy A.G., Gieré R. and Kartashov P.M. (2010) The pyrochlore supergroup of minerals: nomenclature. *The Canadian Mineralogist*, **48**, 673–698.
- Bayliss P., Kaesz H.D. and Nickel E.H. (2005) The use of chemical-element adjectival modifiers in mineral nomenclature. *The Canadian Mineralogist*, **43**, 1429–1433.
- Bonazzi P., Bindi L., Zoppi M., Capitani G.C. and Olmi F. (2006) Single-crystal diffraction and transmission electron microscopy studies of “silicified” pyrochlore from Narssárssuk, Julianehaab district, Greenland. *American Mineralogist*, **91**, 794–801.
- Bosi F., Biagioni C. and Oberti R. (2019a) On the chemical identification and classification of minerals. *Minerals*, **9**, 591.
- Bosi F., Hatert F., Hälenius U., Pasero M., Miyawaki R., and Mills S.J. (2019b) On the application of the IMA–CNMNC dominant-valency rule to complex mineral compositions. *Mineralogical Magazine*, **83**, 627–632.
- Boyle R.W. (1982) Geochemical prospecting for Thorium and Uranium deposits. Pp. 498 in: *Developments in Economic Geology*, Elsevier, Amsterdam.
- Chakhmouradian A.R. and Mitchell R.H. (2002) New data on pyrochlore- and perovskite-group minerals from the Lovozero alkaline complex, Russia. *European Journal of Mineralogy*, **14**, 821–836.
- Chakhmouradian A.R., Reguir E.P., Kressall R.D., Crozier J., Pisiak L.K., Sidhu R. and Yang P. (2015) Carbonatite-hosted niobium deposit at Aley, northern British Columbia (Canada): Mineralogy, geochemistry and petrogenesis. *Ore Geology Reviews*, **64**, 642–666.
- Choisnet J., Nguyen N., Groult D. and Raveau B. (1976) De nouveaux oxydes a reseau forme d'octaedres NbO<sub>6</sub> (TaO<sub>6</sub>) et de groupes Si<sub>2</sub>O<sub>7</sub>: Les phases A<sub>3</sub>Ta<sub>6</sub>Si<sub>4</sub>O<sub>26</sub> (A = Ba, Sr) et K<sub>6</sub>M<sub>6</sub>Si<sub>4</sub>O<sub>26</sub> (M = Nb, Ta). *Materials Research Bulletin*, **11**, 887–894.
- Christy A.G. and Atencio D. (2013) Clarification of status of species in the pyrochlore supergroup. *Mineralogical Magazine*, **77**, 13–20.
- Cooper A.F. (1996) Nb-rich baotite in carbonatites and fenites at Haast River, New Zealand. *Mineralogical Magazine*, **60**, 473–482.
- Dey M., Mitchell R.H., Bhattacharjee S., Chakarabarty A., Pal S., Pal S. and Sen A.K. (2021) Composition and genesis of albitite-hosted antecrystic pyrochlore from the Sevattur carbonatite complex, India. *Mineralogical Magazine*, **85**, <https://doi.org/10.1180/mgm.2021.6>
- Doroshkevich A.G., Viladkar S.G., Ripp G.S. and Burtseva M.V. (2009) Hydrothermal REE mineralization in the Amba Dongar carbonatite complex, Gujarat, India. *The Canadian Mineralogist*, **47**, 1105–1116.



- Doroshkevich A.G., Veksler I.V., Klemd R., Khromova A.E. and Izbrodin, I.A. (2017) Trace element composition of minerals and rocks in the Belaya Zima carbonatite complex (Russia): implications for the mechanisms of magma evolution and carbonatite formation. *Lithos*, **284–285**, 91–108.
- Dumańska-Słowik M., Pieczka A., Tempesta G., Olejniczak Z. and Heflik W. (2014) “Silicified” pyrochlore from nepheline syenite (mariupolite) of the Mariupol Massif, SE Ukraine: A new insight into the role of silicon in the pyrochlore structure. *American Mineralogist*, **99**, 2008–2017.
- Elliott H.A.L., Wall F., Chakhmouradian A.R., Siegfried P.R., Dahlgren S., Weatherley S., Finch A.A., Marks M.A.W., Dowman E. and Deady E. (2018) Fenites associated with carbonatite complexes: A review. *Ore Geology Reviews*, **93**, 38–59.
- Friis H. and Casey W.H. (2018) Niobium is highly mobile as a polyoxometalate ion during natural weathering. *The Canadian Mineralogist*, **56**, 905–912.
- Geisler T., Berndt J., Meyer H.W., Pollok K. and Putnis A. (2004) Low-temperature aqueous alteration of crystalline pyrochlore: correspondence between nature and experiment. *Mineralogical Magazine*, **68**, 905–922.
- Giovannini A.L., Mitchell R.H., Neto A.C.B., Moura C.A., Pereira V.P. and Porto C.G. (2020) Mineralogy and geochemistry of the Morro dos Seis Lagos siderite carbonatite, Amazonas, Brazil. *Lithos*, **360**, 105433.
- Harris P.M. (1965) Pandaite from the Mrima Hill niobium deposit (Kenya). *Mineralogical Magazine*, **35**, 277–290.
- Hatert F. and Burke E.A. (2008) The IMA–CNMNC dominant-constituent rule revisited and extended. *The Canadian Mineralogist*, **46**, 717–728.
- Hogarth D.D. (1977) Classification and nomenclature of the pyrochlore group. *American Mineralogist*, **62**, 403–410.
- Hogarth D.D., Williams C.T. and Jones P. (2000) Primary zoning in pyrochlore group minerals from carbonatites. *Mineralogical Magazine*, **64**, 683–697.
- Jäger E., Niggli E. and Van der Veen A.H. (1959) A hydrated barium-strontium pyrochlore in a biotite rock from Panda Hill, Tanganyika I. *Mineralogical Magazine*, **32**, 10–25.
- Karup-Møller S. (2018) Uranium-rich pyrochlores from the Imaussaq complex, South Greenland. *Neues Jahrbuch für Mineralogie–Abhandlungen/ Journal of Mineralogy and Geochemistry*, **195**, 177–190.
- Kaur G., and Mitchell R.H. (2019) Mineralogy of the baotite-bearing Gundrapalli lamproite, Nalgonda district, Telangana, India. *Mineralogical Magazine*, **83**, 401–411.
- Khromova E.A., Doroshkevich A.G., Sharygin V.V. and Izbrodin L.A. (2017) Compositional evolution of pyrochlore-group minerals in carbonatites of the Belaya Zima Pluton, Eastern Sayan. *Geology of Ore Deposits*, **59**, 752–764.
- Krishnamurthy P. (1977) On some geochemical aspects of the Sevattur carbonatite complex, North Arcot District, Tamil Nadu. *Journal of the Geological Society of India*, **18**, 265–274.
- Krishnamurthy P. (2019) Carbonatites of India. *Journal of the Geological Society of India*, **94**, 117–138.
- Krmičėk L., Cempírek J., Havlín A., Přichystal A., Houzar S., Krmičėková M. and Gadas P. (2011) Mineralogy and petrogenesis of a Ba–Ti–Zr-rich peralkaline dyke from Šebkovic (Czech Republic): recognition of the most lamproitic Variscan intrusion. *Lithos*, **121**, 74–86.
- Kullerud K., Zozulya D., and Ravna E.J. (2012) Formation of baotite—a Cl-rich silicate—together with fluorapatite and F-rich hydrous silicates in the Kvaløya lamproite dyke, North Norway. *Mineralogy and Petrology*, **105**, 145–156.
- Lumpkin G.R. and Ewing R.C. (1995) Geochemical alteration of pyrochlore group minerals: pyrochlore subgroup. *American Mineralogist*, **80**, 732–743.
- Lumpkin G.R. and Ewing R.C. (1996) Geochemical alteration of pyrochlore group minerals: Betafite subgroup. *American Mineralogist*, **81**, 1237–1248.
- Lumpkin G.R., and Mariano A.N. (1995) Natural occurrence and stability of pyrochlore in carbonatites, related hydrothermal systems, and weathering environments. *MRS Online Proceedings Library Archive*, **412**, 831–838.
- Mariano A.N. (1989) Nature of economic mineralization in carbonatites and related rocks. Pp. 149–176 in: *Carbonatites: Genesis and Evolution*. Unwin Hyman, London.
- Melgarejo J.C., Costanzo A., Bambi A.C., Gonçalves A.O. and Neto A.B. (2012) Subsolidus processes as a key factor on the distribution of Nb species in plutonic carbonatites: The Tchivira case, Angola. *Lithos*, **152**, 187–201.
- Migdisov A.A., Boukhalfa H., Timofeev A., Runde W., Roback R. and Williams-Jones A.E. (2018) A spectroscopic study of uranyl speciation in chloride-bearing solutions at temperatures up to 250° C. *Geochimica et Cosmochimica Acta*, **222**, 130–145.
- Mitchell R.H. (2015) Primary and secondary niobium mineral deposits associated with carbonatites. *Ore Geology Reviews*, **64**, 626–641.
- Mitchell R.H. and Smith D.L. (2017) Geology and mineralogy of the Ashram Zone carbonatite, Eldor Complex, Québec. *Ore Geology Reviews*, **86**, 784–806.
- Mitchell R.H., Wahl R. and Cohen A. (2020) Mineralogy and genesis of pyrochlore apatite from The Good Hope Carbonatite, Ontario: A potential niobium deposit. *Mineralogical Magazine*, **84**, 81–91.
- Nasraoui M. and Bilal E. (2000) Pyrochlores from the Lueshe carbonatite complex (Democratic Republic of Congo): a geochemical record of different alteration stages. *Journal of Asian Earth Sciences*, **18**, 237–251.
- Nekrasov J.V., Ponomarev V.I., Simonov V.I. and Kheiker D.M. (1969) A more precise determination of the atomic structure of baotite, and isomorphous relations in this mineral. *Kristallografiya*, **14**, 602–609.
- Nemec D. (1987) Baotite – a rock-forming mineral of Ba-rich hyperpotassic dyke rocks. *Neues Jahrb Mineral Monatshfte*, **1**, 31–42.
- Peng C.J. (1959) The discovery of several new minerals of rare elements. *American Mineralogist*, **45**, 7–45.
- Potter E.G. and Mitchell R.H. (2005) Mineralogy of the Deadhorse Creek volcanoclastic breccia complex, northwestern Ontario, Canada. *Contributions to Mineralogy and Petrology*, **150**, 212–229.
- Pressacco R. (2001) Geology of the Cargill Township Residual Carbonatite-associated Phosphate Deposit, Kapuskasing, Ontario. *Exploration and Mining Geology*, **10**, 77–84.
- Ramasamy R., Gwalani L.G. and Subramanian S.P. (2001) A note on the occurrence and formation of magnetite in the carbonatites of Sevattur, North Arcot district, Tamil Nadu, Southern India. *Journal of Asian Earth Sciences*, **19**, 297–304.
- Rukhlov A.S. and Bell K. (2010) Geochronology of carbonatites from the Canadian and Baltic Shields, and the Canadian Cordillera: clues to mantle evolution. *Mineralogy and Petrology*, **98**, 11–54.
- Schleicher H. (2019) In-situ determination of trace element and REE partitioning in a natural apatite-carbonatite melt system using synchrotron XRF microprobe analysis. *Journal of the Geological Society of India*, **93**, 305–312.
- Schleicher H., Kramm U., Pernicka E., Schidlowski M., Schmidt F., Subramanian V., Todt W. and Viladkar S.G. (1998) Enriched subcontinental upper mantle beneath southern India: evidence from Pb, Nd, Sr, and C–O isotopic studies on Tamil Nadu carbonatites. *Journal of Petrology*, **39**, 1765–1785.
- Semenov E.I., Khun V.S. and Kapitonova T.A. (1961) Baotite, a new niobian mineral. *Doklady AN USSR*, **136**, 915–916 [in Russian].
- Sharygin V.V., Sobolev N.V. and Channer D.M.D. (2009) Oscillatory-zoned crystals of pyrochlore-group minerals from the Guaniamo kimberlites, Venezuela. *Lithos*, **112**, 976–985.
- Sorokhtina N.V., Voloshin A.V. and Pakhomovsky Ya.A. (1998) Belkovite from calcite-dolomite carbonatites of the Sebljavr massif (Kola Peninsula). *Zapiski Vserossiiskogo Mineralogicheskogo Obshchestva*, **127**, 79–84 [in Russian].
- Sorokhtina N.V., Kogarko L.N. and Shpachenko A.K. (2010) New data on mineralogy and geochemistry of rare-metal mineralization of the Gremiakha-Vyrmes Massif. *Doklady Earth Sciences*, **434**, 243–247.
- Subramanian V., Viladkar S.G. and Upendran R. (1978) Carbonatite alkali complex of Samalpatti, Dharmapuri district, Tamil Nadu. *Journal of the Geological Society of India*, **19**, 206–216.
- Timofeev A. and Williams-Jones A.E. (2015) The origin of niobium and tantalum mineralization in the Nechalacho REE Deposit, NWT, Canada. *Economic Geology*, **110**, 1719–1735.
- Timofeev A., Migdisov A.A., and Williams-Jones A.E. (2017) An experimental study of the solubility and speciation of tantalum in fluoride-bearing aqueous solutions at elevated temperature. *Geochimica et Cosmochimica Acta*, **197**, 294–304.
- Timofeev A., Migdisov A.A., Williams-Jones A.E., Roback R., Nelson A.T. and Xu H. (2018) Uranium transport in acidic brines under reducing conditions. *Nature communications*, **9**, 1–7.

- Traversa G., Gomes C.B., Brotzu P., Buraglini N., Morbidelli L., Principato M.S., Ronca S. and Ruberti E. (2001) Petrography and mineral chemistry of carbonatites and mica-rich rocks from the Araxá complex (Alto Paranaíba Province, Brazil). *Anais da Academia Brasileira de Ciências*, **73**, 71–98.
- Udas G.R. and Krishnamurthy P. (1970) Carbonatites of Sevathur and Jokipatti, Madras State, India. *Proceedings of Indian National Science Academy*, **36**, 331–343.
- Uher P., Černý P., Chapman R., Hatar J. and Miko O. (1998) Evolution of Nb, Ta-oxide minerals in the Prašivá granitic pegmatites, Slovakia. II. External hydrothermal Pb,Sb overprint. *The Canadian Mineralogist*, **36**, 535–545.
- Viladkar S.G. and Bismayer U. (2010) Compositional variation in pyrochlores of Amba Dongar carbonatite complex, Gujarat. *Journal of the Geological Society of India*, **75**, 495–502.
- Viladkar S.G. and Bismayer U. (2014) U-rich pyrochlore from Sevathur carbonatites, Tamil Nadu. *Journal of the Geological Society of India*, **83**, 175–182.
- Viladkar S.G. and Subramanian V. (1995) Mineralogy and geochemistry of the carbonatites of the Sevathur and Samalpatti complexes, Tamil-Nadu. *Journal of the Geological Society of India*, **45**, 505–517.
- Voloshin A.V., Pakhomovsky Y.A., Pushcharovsky D.Y., Nadezhina T.N., Bakhchisaraitsev A.Y. and Kobayashv Y.S. (1989) Strontio-pyrochlore: composition and structure. *Trudy Mineralogicheskogo Muzeya AN SSSR*, **36**, 12–24 [in Russian].
- Voloshin A.V., Subbotin V.V., Pakhomovsky Y.A., Bakhchisaraitsev A.Y., Yamnova N.A. and Pushcharovsky D.Y. (1990) Belkovite  $Ba_2(Nb, Ti)_6(Si_2O_7)_2O_{12}$ . A new mineral from carbonatite of the Vuoriyarvi pluton (Kola Peninsula). *Transactions (Doklady) of the USSR Academy of Sciences. Earth Science Sections*, **315**, 229–232.
- Voloshin A.V., Subbotin V.V., Pakhomovsky Y.A., Bakhchisaraitsev A.Y. and Yamnova N.A. (1991) Belkovite – a new barium-niobium silicate from carbonatites of the Vuoriyarvi massif (Kola Peninsula, USSR). *Neues Jahrbuch für Mineralogie Monatshefte*, **1**, 23–31.
- Wall F., Williams C.T., Woolley A.R. and Nasraoui M. (1996) Pyrochlore from weathered carbonatite at Lueshe, Zaire. *Mineralogical Magazine*, **60**, 731–750.
- Walter B.F., Parsapoor A., Braunger S., Marks M.A.W., Wenzel T., Martin M. and Markl G. (2018) Pyrochlore as a monitor for magmatic and hydrothermal processes in carbonatites from the Kaiserstuhl volcanic complex (SW Germany). *Chemical Geology*, **498**, 1–16.
- Williams C.T., Wall F., Woolley A.R. and Phillipso S. (1997) Compositional variation in pyrochlore from the Bingo carbonatite, Zaire. *Journal of African Earth Sciences*, **25**, 137–145.
- Zurevinski S.E. and Mitchell R.H. (2004) Extreme compositional variation of pyrochlore-group minerals at the Oka carbonatite complex, Quebec: evidence of magma mixing? *The Canadian Mineralogist*, **42**, 1159–1168.